

Modulating the spin-flip rates and emission energy through ligand design in chromium(III) molecular rubies

Yating Ye,^a Maxime Poncet,^b Polina Yaltseva,^c Pablo Salcedo-Abraira,^a Antonio Rodríguez-Diéquez,^a Javier Heredia Martín,^a Laura Cuevas-Contreras,^a Carlos M. Cruz,^d Benjamin Doistau,^e Claude Piguet,^b Oliver S. Wenger,^c Juan Manuel Herrera,^a and Juan-Ramón Jiménez^{*a}

-
- ^a. Department of Inorganic Chemistry. University of Granada and “Unidad de Excelencia en Química (UEQ)”, Avda. Fuente Nueva s/n, 18071, Granada, Spain.
 - ^b. Department of Analytical and Inorganic Chemistry. University of Geneva. 30 quai Ernest Ansermet, CH-1211 Geneva 4, Switzerland.
 - ^c. Department of Chemistry, University of Basel, St. Johanns-Ring 19, 4056, Basel, Switzerland
 - ^d. Department of Organic Chemistry. University of Granada and “Unidad de Excelencia en Química (UEQ)”, Avda. Fuente Nueva s/n, 18071, Granada, Spain.
 - ^e. Laboratoire de Chimie et de Biochimie Pharmacologiques et Toxicologiques, Université Paris Cité, CNRS, 45 rue des Saint-Pères F-75006 Paris, France.

Supporting Information

(51 pages)

Experimental part

Elemental analyses were carried out on a Fisons-Carlo Erba analyser model EA 1108. ^1H Nuclear Magnetic Resonance Spectroscopy (RMN) data were recorded on a 400 MHz BRUKER Nanobay Avance III HD High-Definition spectrometer and the spectra were internally referenced to solvent signals. Cyclic Voltammetry measurements were conducted in a one-compartment three-electrode cell for 0.15 mM analyte solutions in acetonitrile. $^{\text{n}}\text{BuN}_4\text{PF}_6$ was utilized as the supporting electrolyte with a solution concentration of 0.1 M. Glassy carbon (3 mm diameter) was employed as the working electrode while Pt wire was utilized as the counter electrode and Ag/AgCl (5mM) as reference electrode. Absorption spectra in acetonitrile solution were recorded using a Jasco Cary (Agilent Technologies) spectrometer (quartz cell path length 1 cm or 1 mm, 290-800 nm domain, 2×10^{-4} M and 650-800 nm domain, 7.7 mM). Emission and excitation spectra were measured on a UV-VIS-PTI QuantaMasterTM 8000 spectrofluorometer equipped with a Picosecond Photon Detector (230-850nm, PPD-850, HORIBA Scientific) and a continuous Xenon Short Arc Lamp (190-2000nm, USHIO). All the spectra (emission and excitation) were corrected with real-time correction functions. Time Correlated Single Photon Counting (TCSPC) lifetime measurements were performed using a 480 nm or 450 nm flash lamp (1 μs pulse, HORIBA Scientific). Low temperature (77 K) was achieved using liquid quartz transparent Dewar filled with liquid N₂ in the center of which samples were placed. Sample solutions in CH₃CN, were introduced in quartz tube (4 mm interior diameter) and introduced into the sample holder of the Dewar. All emission luminescence quantum yields were measured according to an absolute method which makes use of an integration sphere. Mass spectrometry measurements have been recorded in a Compact Bruker QTOF with UHPLC Elute Ole Bruker. Using the relationship $k_q = 1/[\text{O}_2] \cdot (1/\tau_{\text{air}} - 1/\tau_{\text{Ar}})$, where [O₂] is the oxygen concentration (2.42 mM in CH₃CN at 20 °C), τ_{air} is the $^2\text{E}/^2\text{T}_1$ lifetime under aerated conditions and τ_{Ar} the respective lifetime under deaerated condition, k_q values for energy transfer from $^2\text{E}/^2\text{T}_1$ to O₂ could be estimated (see main text). UV-vis transient absorption measurements on the nanosecond timescale were carried out on an LP920-KS instrument from Edinburgh Instruments. A frequency-tripled pulsed Nd:YAG laser (Quantel Q-smart 450, ca. 10 ns pulse width) with a beam expander (BE02-355 from Thorlabs) in the beam path was used for excitation at 355 nm (pulse energy of ~30 mJ) and a frequency-tripled Nd:YAG laser (Quantel Brilliant, ca. 10 ns pulse width) equipped with OPO from Opotek

and a beam expander (GBE02-A from Thorlabs) in the beam path was used for excitation at 450 nm (pulse energy of ~13 mJ). An iCCD camera from Andor was used to detect transient absorption spectra, and single-wavelength kinetics were recorded with a photomultiplier tube (Hamamatsu).

X-Ray Crystallography.

Suitable crystals of **1**, **2** and **3** were mounted on a Bruker D8 Venture diffractometer. Details of the crystals, data collection and refinement parameters are given in Table S1. After data processing (raw data integration, merging of equivalent reflections and absorption correction), the structures were solved by direct or Patterson methods and refined using least squares minimization with the SHELX suite of programs^[S1] integrated in OLEX2.^[S2] Selected bonds and lengths are given in Tables S2 and S3. In **2**, the iodine atom I1 is disordered over two sites and refined with site occupancies of 0.5/0.5. Carbon atoms C1S and C3S, which belong to a diethyl ether solvation molecule, are also disordered. The checkcif file of this structure contains two A-level alerts associated with residual peaks near a triflate counterion which is probably disordered and which we could not model. The CCDC numbers 2266702 (**1**), 2266703 (**2**) and (**3**) 2389781 contain the supplementary crystallographic data for this article. These data are provided free of charge by the Cambridge Crystallographic Data Centre.

Appendix. Experimental section.

Solvents and starting materials

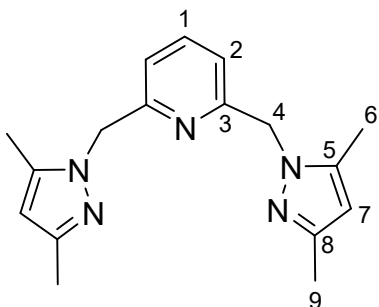
All the chemicals were purchased from commercial suppliers and used without further purification.

Synthesis: Preparation of the ligands and complexes

Synthesis of 2,6-bis((3,5-dimethyl-1H-pyrazol-1-yl)methyl)pyridine (Mebipzp) and 2,6-bis((4-iodo-3,5-dimethyl-1H-pyrazol-1-yl)methyl)pyridine (IMebipzp) and 2,6-bis(indazol-2-ylmethyl)pyridine (bip).

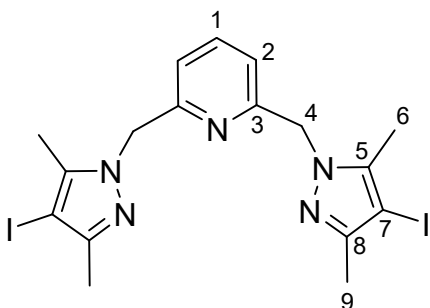
In a 100 mL round-bottom flask containing 20 mL of toluene were added: 0.3050 g of 2,6-bis(chloromethyl)pyridine and 0.3345 g of 3,5-dimethylpyrazole for Mebipzp or 0.3060 of 3,5-dimethyl-4-iodo-pyrazole for IMebipzp. On the other hand, a 40% NaOH solution was prepared, containing 4.8 g of NaOH dissolved in 12 mL of water, and 10 drops of TBAOH were added. This basic solution was added to the pyrazole containing

solution which was subsequently refluxed at 110°C for 24 hours. After this period, the mixture was allowed to cool to room temperature, and a liquid-liquid extraction was performed to separate the organic phase (toluene). The organic phase was washed with 3x10 mL of water. The organic phase was then dried with MgSO₄, filtered, and the solvent was removed under vacuum, resulting in the desired product in the form of a white solid (reaction yield: 90%).



¹H-NMR (400 MHz, CDCl₃, ppm) δ: 7.53-7.49 (t, *J* = 7.8 Hz, 1H), 6.64-6.62 (d, *J* = 7.8 Hz, 2H), 5.87 (s, 2H), 5.30 (s, 4H), 2.30 (s, 6H), 2.19 (s, 6H). ¹³C NMR (CD₃CN) δ = 158.28 (C3), 148.21 (C8), 140.80 (C5), 138.85 (C1), 120.93 (C2), 105.99 (C7), 54.75 (C4), 13.55 (C9), 11.19 (C6).

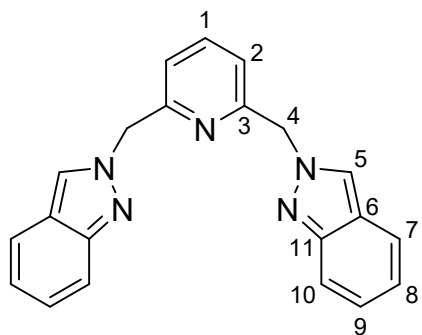
ESI-MS (m/z): 296.2 [L+H]⁺.



¹H-NMR (400 MHz, CDCl₃, ppm) δ: 7.55 (t, *J* = 7.8 Hz, 1H), 6.77 (d, *J* = 7.8 Hz 2H), 5.35 (s, 4H), 2.25 (s, 6H), 2.2 (s, 6H). ¹³C NMR (CDCl₃) δ = 156.26 (C3), 149.84 (C8), 141.31 (C5), 138.12 (C1), 119.96 (C2), 63.22 (C7), 55.33 (C4), 13.98 (C6), 11.91 (C9).

ESI-MS (m/z): 569.9 [L+Na]⁺.

For the synthesis of 2,6-bis(indazol-2-ylmethyl)pyridine (bip), we use 2,6-bis(bromomethyl)pyridine (0.300 g, 1.132 mmol) instead of 2,6-bis(chloromethyl)pyridine with 1H-indazole (0.267 g, 2.264 mmol). The synthesis procedure is the same as Mebipzp and IMebipzp (reaction yield: 80%).



¹H-NMR (400 MHz, CDCl₃, ppm) δ: 8.04 (s, 2H), 7.79 – 7.64 (m, 4H), 7.60 – 7.44 (m, 1H), 7.30 (t, *J* = 1.1, 2H), 7.10 (t, *J* = 0.9, 2H), 6.97 (d, *J* = 7.8, 2H), 5.72 (s, 4H). ¹³C-NMR (CD₃CN) δ = 156.35 (C11), 149.39, 138.58, 126.89 (C3, C1, C9), 124.82 (C5), 121.92 (C6), 121.50 (C8), 121.19 (C7), 120.98, 117.75 (C2, C10), 58.90 (C4).

ESI-MS (m/z): 362.1 [L+Na]⁺.

Synthesis of [Cr(Mebipzp)₂](SO₃CF₃)₃ (**1**) and [Cr(IMebipzp)₂](SO₃CF₃)₃ (**2**) [Cr(bip*)₂](SO₃CF₃)₃ (**3**)

In a glovebox 2 mmol of ligand suspended in 10 mL of anhydrous acetonitrile were added dropwise to a solution containing 1 mmol of Cr(CF₃SO₃)₂·2H₂O previously dissolved in 5 mL of anhydrous acetonitrile. The mixture was stirred for 2 h at 35°C resulting in a purple solution. Subsequent addition of 1 mmol of AgSO₃CF₃ led to a colour change from purple to orange with the apparition of a grey solid. The mixture was stirred for additional 4 h. The reaction was taken from the glovebox and filtered through a membrane of PTFE of 2 μm. The volume of the orange solution was reduced under vacuum and diethyl ether was added to precipitate the solids which were filtered giving a pale pink solid for **1**, an orange solid for **2** and an orange solid for **3** (reaction yields >90%). Elemental analysis for **1**: C₃₇H₄₂CrF₉N₁₀O₉S₃P₃·1.8H₂O %, found: C: 39.75, N: 12.59, H: 3.75; calculated: C: 40.01, N: 12.61, H: 4.02. Elemental analysis for **2**: C₃₇H₃₈CrF₉I₄N₁₀O₉S₃P₃·H₂O, found %: C: 27.26, N: 8.53, H: 2.49; calculated: C: 27.33, N: 8.61, H: 2.58. Elemental analysis for **3**: C₄₅H₃₄CrF₉N₁₀O₉S₃·0.9 H₂O %, found: C: 45.13, H: 2.87, N: 11.63; calculated: C: 45.26, H: 3.02, N: 11.73.

Single crystals suitable for X-ray diffraction were obtained by slow diffusion of diethyl ether into a concentrated acetonitrile solution containing the complexes after 48 h.

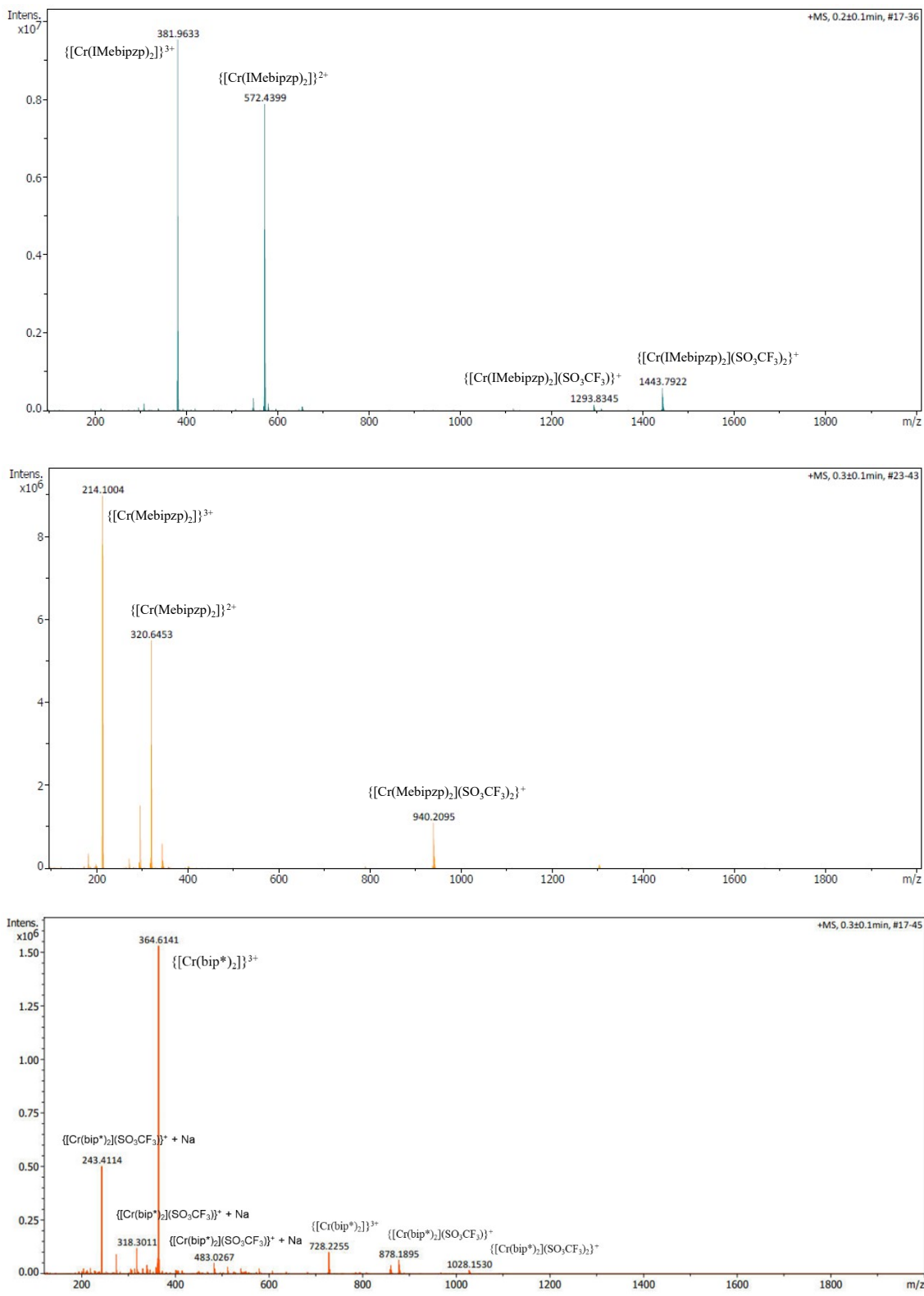


Figure S1. ESI-Mass spectrometry for complex **1** (top), **2** (medium) and **3** (bottom) and their respective assignation.

Table S1. Crystallographic data for complexes **1**, **2** and **3**

	1	2
Empirical formula	C ₄₁ H ₄₈ CrF ₉ N ₁₂ O ₉ S ₃	C ₄₃ H ₅₁ CrF ₉ I ₄ N ₁₁ O ₁₀ S ₃
Formula weight	1172.09	1708.72
Crystal system	monoclinic	monoclinic
Space group	<i>P</i> 2 ₁ / <i>c</i>	<i>P</i> 2 ₁ / <i>n</i>
a/Å	21.2505(15)	11.8195(5)
b/Å	11.5885(7)	22.8812(10)
c/Å	20.6086(13)	22.7016(10)
β/°	92.210(2)	100.6638(16)
Volume/Å ³	5071.3(6)	6033.5(5)
Z	4	4
ρ _{calc} g/cm ³	1.535	1.881
μ/mm ⁻¹	0.447	2.428
F(000)	2412.0	3324.0
Crystal size/mm ³	0.243 × 0.216 × 0.026	0.247 × 0.101 × 0.051
Radiation	MoKα (λ = 0.71073)	MoKα (λ = 0.71073)
2Θ range for data collection/°	3.956 to 56.726	3.932 to 56.606
	-28 ≤ h ≤ 28,	-15 ≤ h ≤ 15,
Index ranges	-14 ≤ k ≤ 15, -27 ≤ l ≤ 27	-30 ≤ k ≤ 30, -28 ≤ l ≤ 30
Reflections collected	79343	92085
Independent reflections	12613 [R _{int} = 0.0398, R _{sigma} = 0.0284]	14938 [R _{int} = 0.0548, R _{sigma} = 0.0369]
Data/restraints/parameters	12613/0/686	14938/95/772
Goodness-of-fit on F ²	1.053	1.073
Final R indexes [I>=2σ (I)]	R ₁ = 0.0413, wR ₂ = 0.1091	R ₁ = 0.0611, wR ₂ = 0.1405
Final R indexes [all data]	R ₁ = 0.0500, wR ₂ = 0.1165	R ₁ = 0.0816, wR ₂ = 0.1539
Largest diff. peak/hole / e Å ⁻³	1.26/-0.72	3.10/-1.54

3

Empirical formula	C ₄₅ H ₅₄ CrF ₉ N ₁₀ O ₁₉ S ₃
Formula weight	1358.16
Temperature/K	100.00
Crystal system	orthorhombic
Space group	<i>Pna</i> 2 ₁
a/Å	24.8078(9)
b/Å	21.0257(10)
c/Å	11.4987(5)
$\alpha/^\circ$	90
$\beta/^\circ$	90
$\gamma/^\circ$	90
Volume/Å ³	5997.7(4)
Z	4
ρ_{calc} g/cm ³	1.504
μ/mm^{-1}	0.400
F(000)	2796.0
Crystal size/mm ³	0.246 × 0.221 × 0.216
Radiation	MoKα ($\lambda = 0.71073$)
2Θ range for data collection/°	3.812 to 50.054
Index ranges	-28 ≤ h ≤ 29, -25 ≤ k ≤ 25, -13 ≤ l ≤ 13
Reflections collected	49184
Independent reflections	10588 [R _{int} = 0.0473, R _{sigma} = 0.0293]
Data/restraints/parameters	10588/1284/654
Goodness-of-fit on F ²	1.687
Final R indexes [I>=2σ (I)]	R ₁ = 0.1037, wR ₂ = 0.3308
Final R indexes [all data]	R ₁ = 0.1117, wR ₂ = 0.3517
Largest diff. peak/hole / e Å ⁻³	2.19/-1.23
Flack parameter	0.51(6)

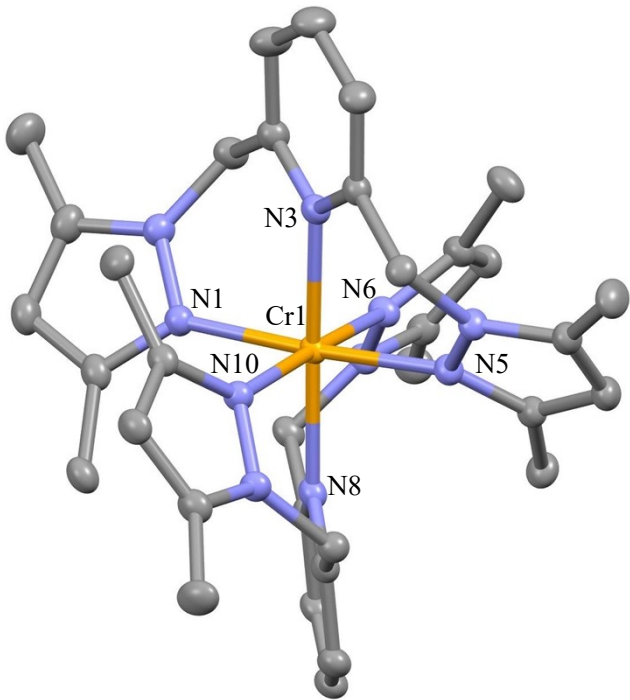


Figure S2. Molecular Structure of 1. Colour codes: Cr (orange), N (blue), C (grey).

Table S2. Selected bond distances (\AA) and angles ($^{\circ}$) for complex 1

Bond distances (\AA)		Bond angles ($^{\circ}$)	
Cr1-N1	2.0527(15)	N1-Cr1-N3	88.63(6)
Cr1-N3	2.0813(14)	N1-Cr1-N5	176.25(6)
Cr1-N5	2.0634(15)	N1-Cr1-N6	92.89(6)
Cr1-N6	2.0550(14)	N1-Cr1-N8	93.38(6)
Cr1-N8	2.0869(14)	N1-Cr1-N10	85.80(6)
Cr1-N10	2.0470(14)	N3-Cr1-N5	87.82(6)
		N3-Cr1-N6	93.28(6)
		N3-Cr1-N8	177.28(6)
		N3-Cr1-N10	90.36(6)
		N5-Cr1-N6	86.11(6)
		N5-Cr1-N8	90.20(6)
		N5-Cr1-N10	95.43(6)
		N6-Cr1-N8	88.44(6)
		N6-Cr1-N10	176.10(6)
		N8-Cr1-N10	87.97(6)

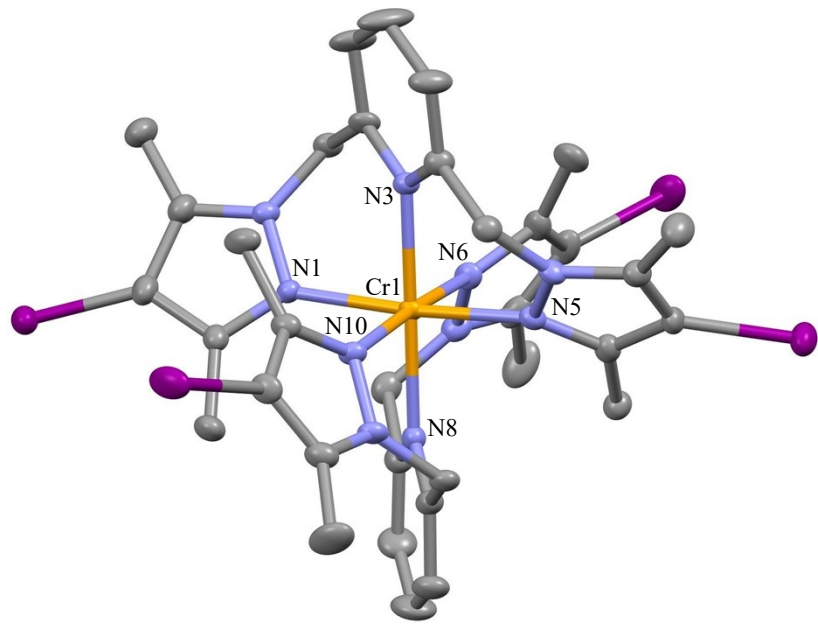


Figure S3. Molecular Structure of **2**. Colour codes: Cr (orange), N (blue), C (grey), I (purple).

Table S3. Selected bond distances (\AA) and angles ($^{\circ}$) for complex **2**

Bond distances (\AA)		Bond angles ($^{\circ}$)	
Cr1-N1	2.067(5)	N1-Cr1-N3	87.28(18)
Cr1-N3	2.091(5)	N1-Cr1-N5	175.28(19)
Cr1-N5	2.065(5)	N1-Cr1-N6	93.53(19)
Cr1-N6	2.065(5)	N1-Cr1-N8	92.69(18)
Cr1-N8	2.104(5)	N1-Cr1-N10	86.51(19)
Cr1-N10	2.069(5)	N3-Cr1-N5	88.06(18)
		N3-Cr1-N6	92.80(19)
		N3-Cr1-N8	178.97(19)
		N3-Cr1-N10	91.38(18)
		N5-Cr1-N6	85.95(19)
		N5-Cr1-N8	91.99(18)
		N5-Cr1-N10	94.36(19)
		N6-Cr1-N8	88.23(19)
		N6-Cr1-N10	175.8(2)
		N8-Cr1-N10	87.59(18)

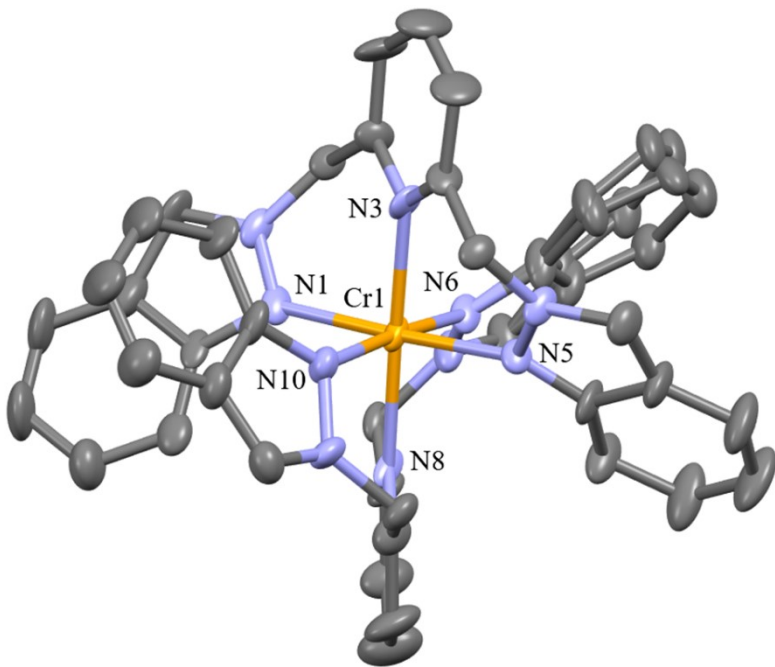


Figure S4. Molecular Structure of **3**. Colour codes: Cr (orange), N (blue), C (grey), I (purple).

Table S4. Selected bond distances (\AA) and angles ($^{\circ}$) for complex **3**

	Bond distances (\AA)	Bond angles ($^{\circ}$)
Cr1-N3	2.079(7)	N3-Cr1-N8 178.5(2)
Cr1-N5	2.043(6)	N5-Cr1-N3 88.5(3)
Cr1-N10	2.030(7)	N5-Cr1-N8 90.0(2)
Cr1-N1	2.047(6)	N10-Cr1-N3 91.7(3)
Cr1-N8	2.098(4)	N10-Cr-N5 95.0(3)
Cr1-N6	1.999(7)	N10-Cr-N1 85.7(2)
		N10-Cr1-N8 88.0(3)
		N1-Cr1-N3 88.8(3)
		N1-Cr1-N5 177.3(3)
		N1-Cr1-N8 92.6(2)
		N6-Cr1-N3 92.9(3)
		N6-Cr1-N5 85.2(2)
		N6-Cr1-N10 175.4(3)
		N6-Cr1-N1 94.4(3)
		N6-Cr-N8 87.3(3)

Table S5. SHAPE analysis of the compounds $[\text{Cr}(\text{bpmp})_2]^{3+}$, $[\text{Cr}(\text{btmp})_2]^{3+}$, **1, **2** and **3****

	JPPY-6	TPR-6	OC-6	PPY-6	HP-6
$[\text{Cr}(\text{bpmp})_2]^{3+}$	31.949	15.635	0.158	28.611	31.107
$[\text{Cr}(\text{btmp})_2]^{3+}$	32.182	15.898	0.151	28.855	30.753
1	31.175	14.327	0.186	27.654	31.836
2	31.272	14.843	0.183	27.77	31.885
3	31.075	14.859	0.208	27.818	31.59

JPPY-6 5 C5v Johnson pentagonal pyramid J2

TPR-6 4 D3h Trigonal prism

OC-6 3 Oh Octahedron

PPY-6 2 C5v Pentagonal pyramid

HP-6 1 D6h Hexagon

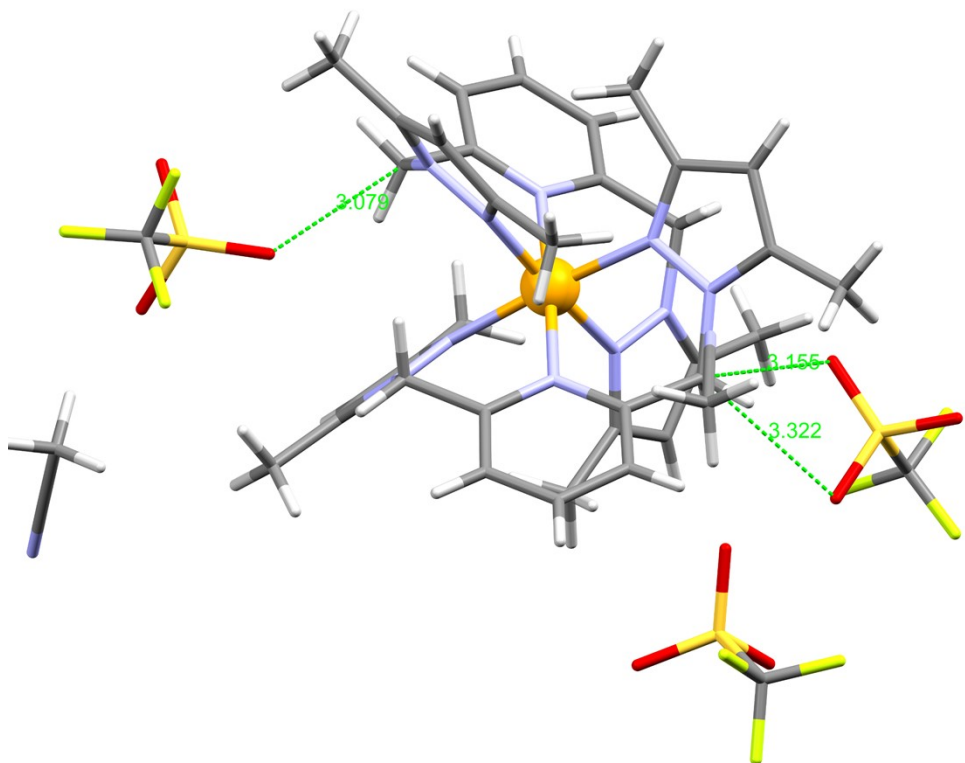


Figure S5. Molecular Structure of **1**. Colour codes: Cr (orange), N (blue), C (grey), H (white), F (green), S (yellow) and O (red).

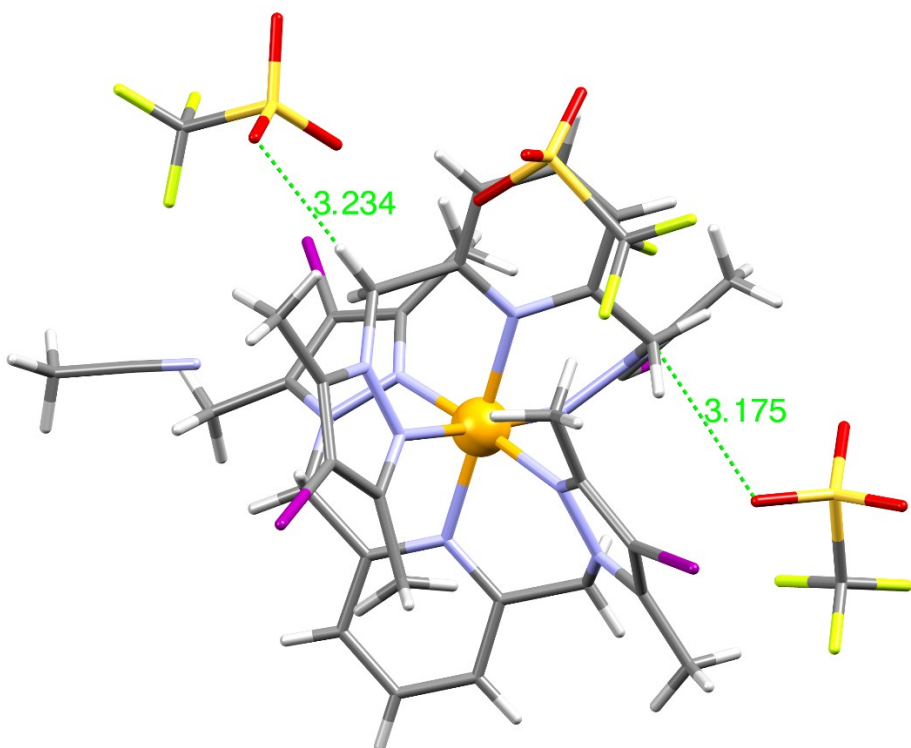


Figure S6. Molecular Structure of **2**. Colour codes: Cr (orange), N (blue), C (grey), H (white), I (purple), F (green), S (yellow) and O (red).

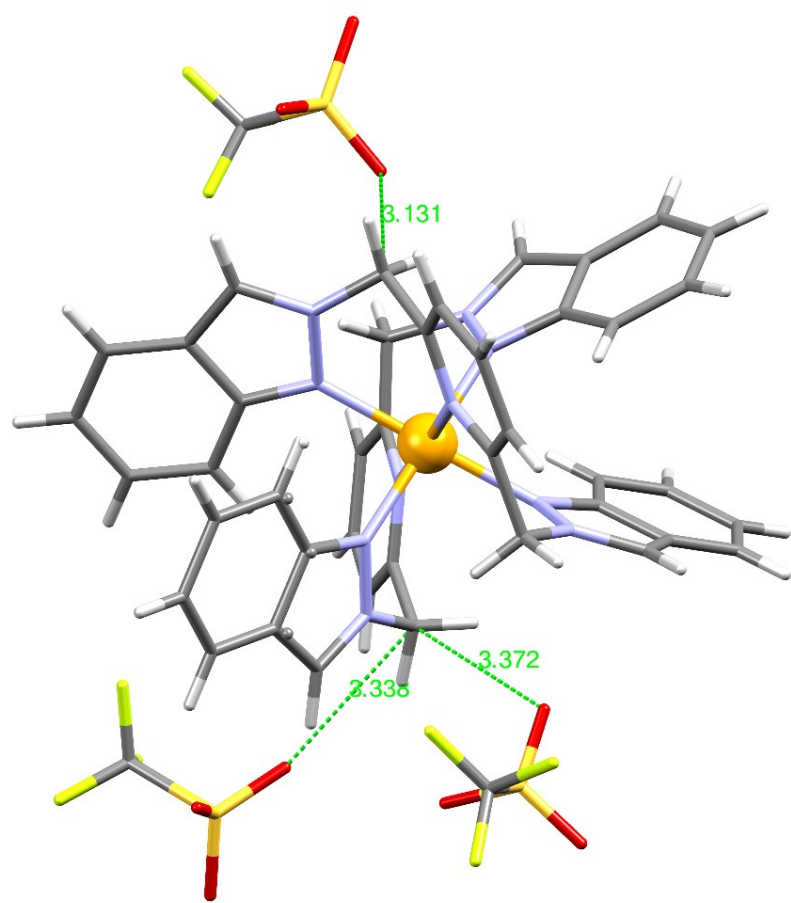


Figure S7. Molecular Structure of **3**. Colour codes: Cr (orange), N (blue), C (grey), H (white), F (green), S (yellow) and O (red).

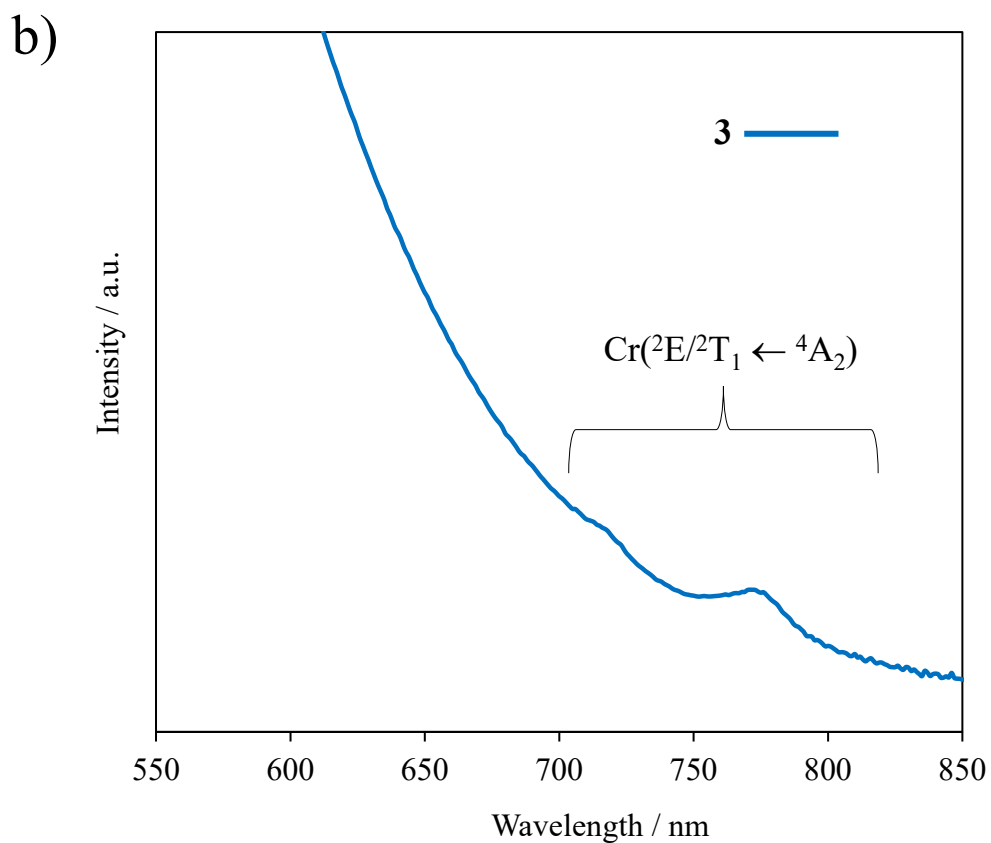
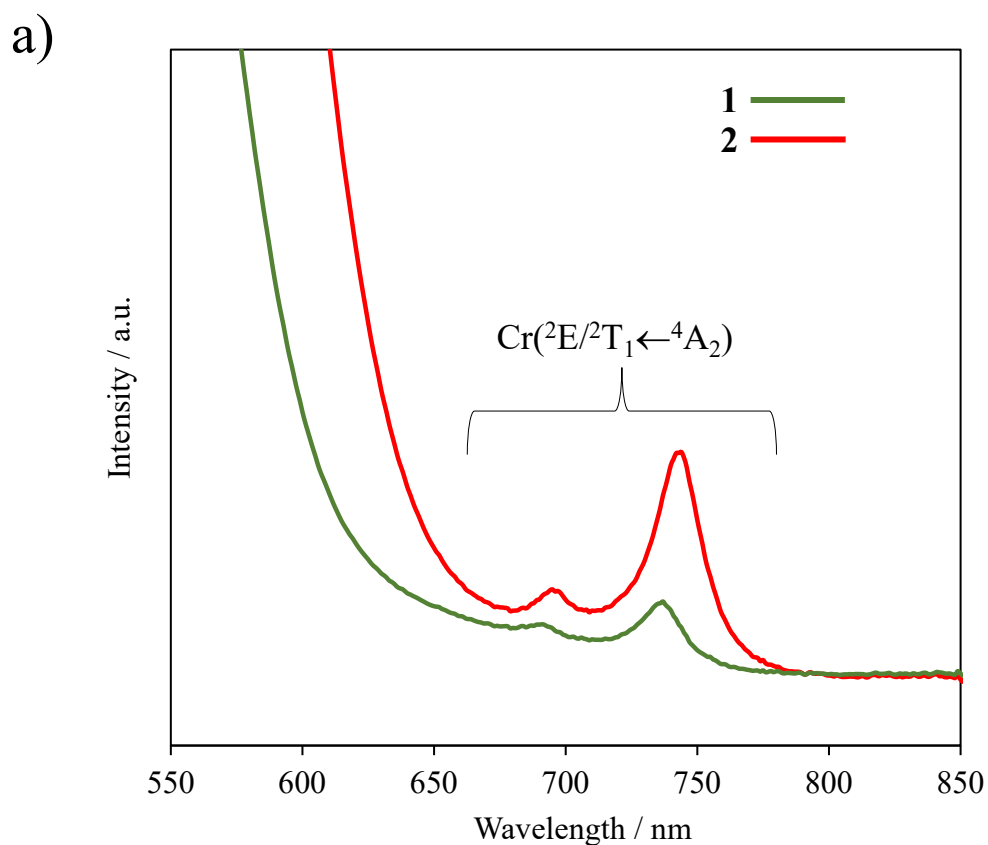


Figure S8. a) Solid state absorption spectra of $[\text{Cr}(\text{Mebipzp})_2]^{3+}$ (**1**) and $[\text{Cr}(\text{IMebipzp})_2]^{3+}$ (**2**), and b) $[\text{Cr}(\text{bip}^*)_2]^{3+}$ (**3**)

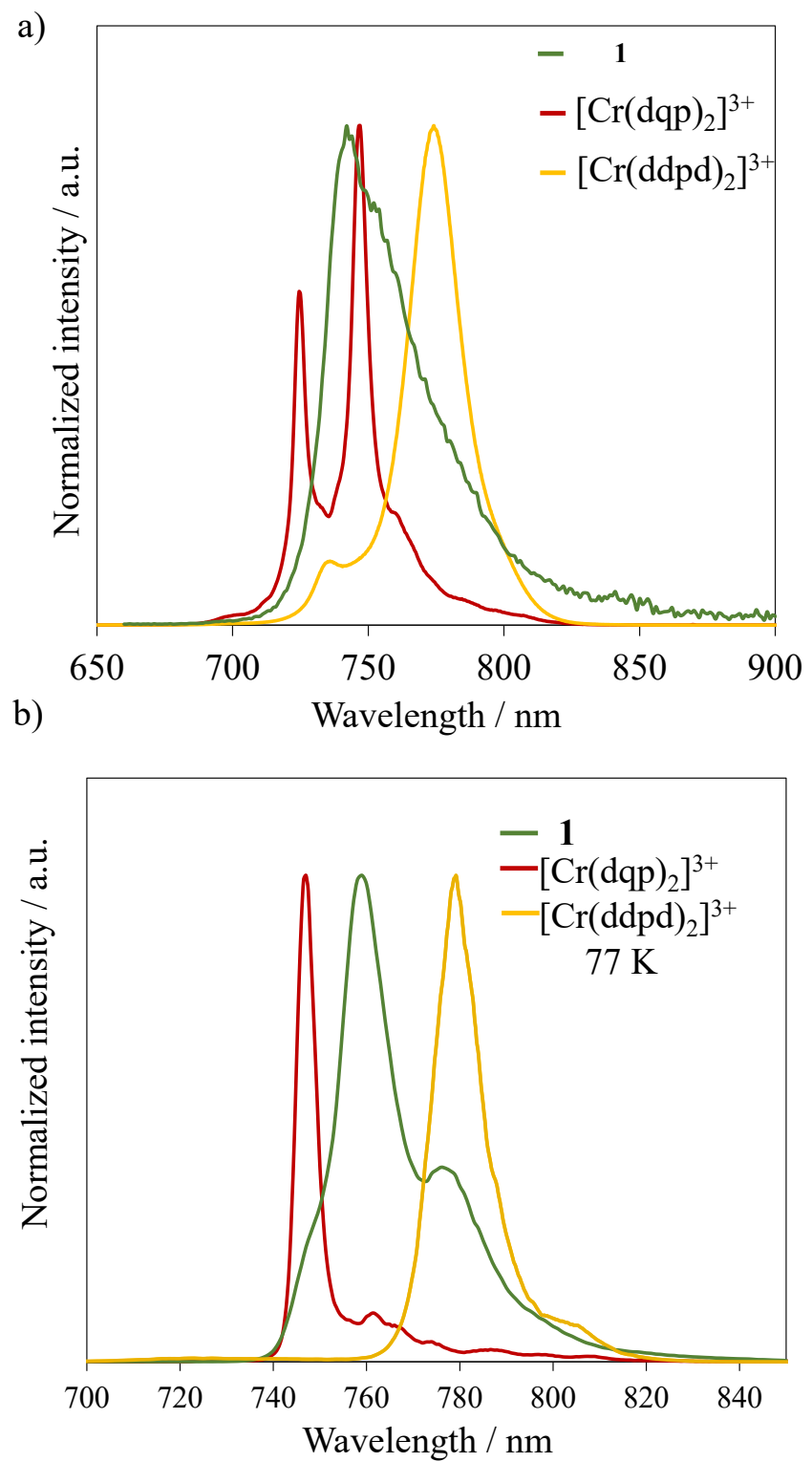


Figure S9. Comparison of emission spectra of $\text{---} \textcolor{green}{\text{l}}$, $[\text{Cr}(\text{dqp})_2]^{3+}$ and $[\text{Cr}(\text{ddpd})_2]^{3+}$ at room temperature (a) and 77 K in frozen solution (b).

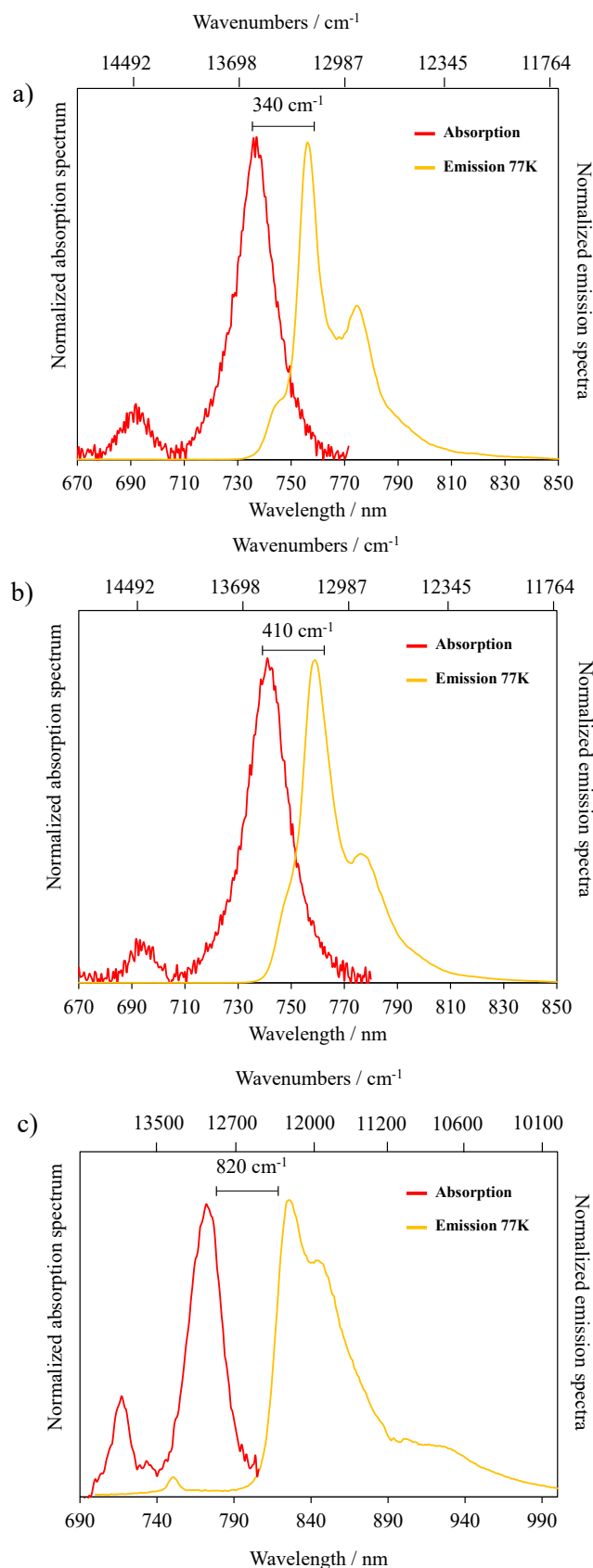


Figure S10. Comparison of absorption and emission spectra at 77 K for complex **1** (a), **2** (b) and **3** (c).

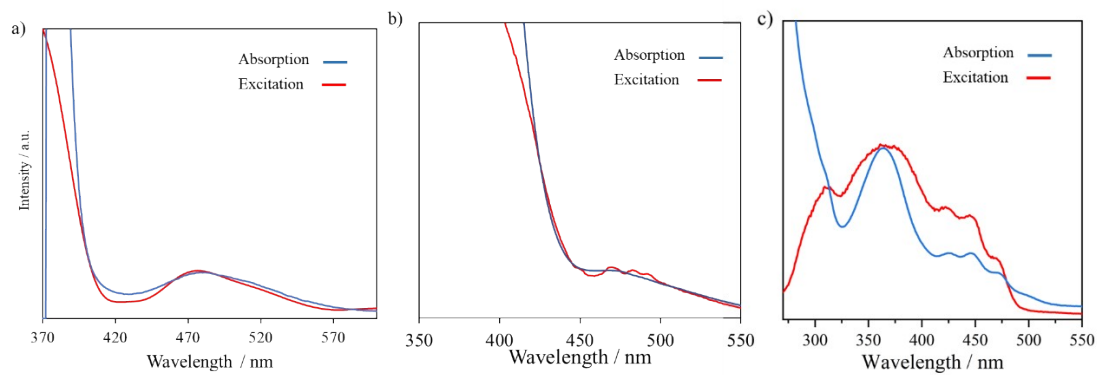


Figure S11. Excitation spectra of **1** (a), **2** (b), upon monitoring $\lambda_{\text{em}} = 748$ nm and **3** (c) monitored at $\lambda_{\text{em}} = 830$ nm.

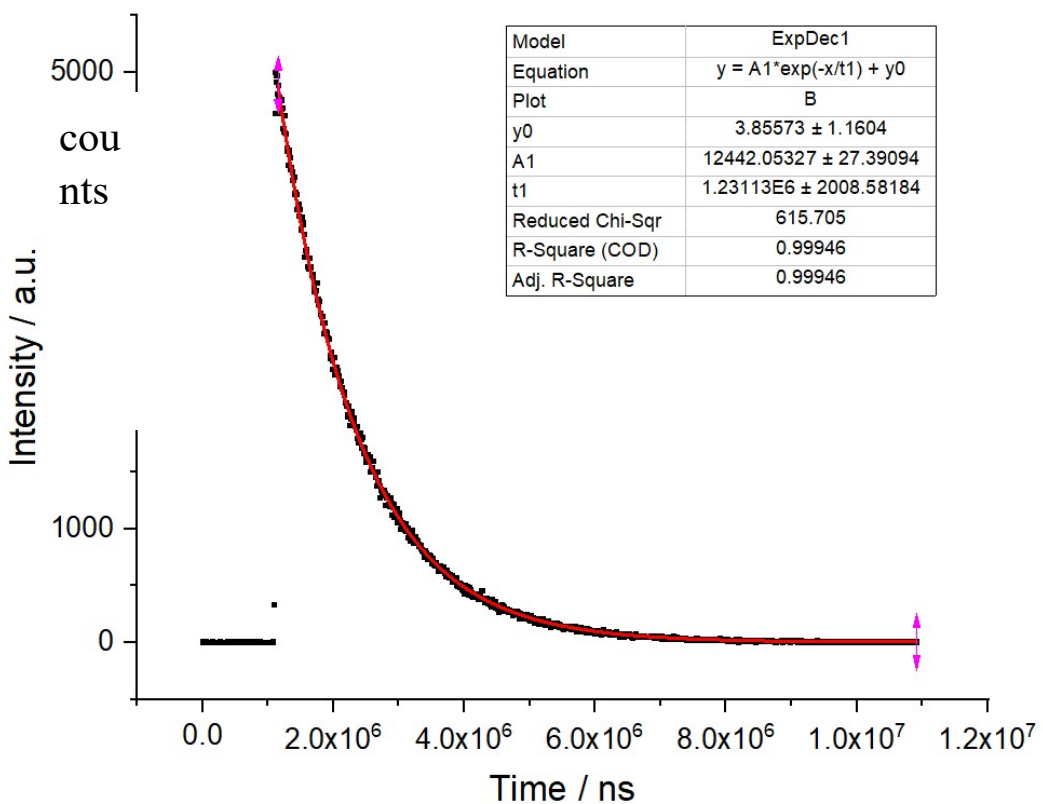


Figure S12. Excited state lifetime and the best fit of the experimental data for the $[\text{Cr}(\text{Mebipzp})_2]^{3+}$ complex ($\lambda_{\text{exc}} = 480$ nm) in deaerated acetonitrile solution

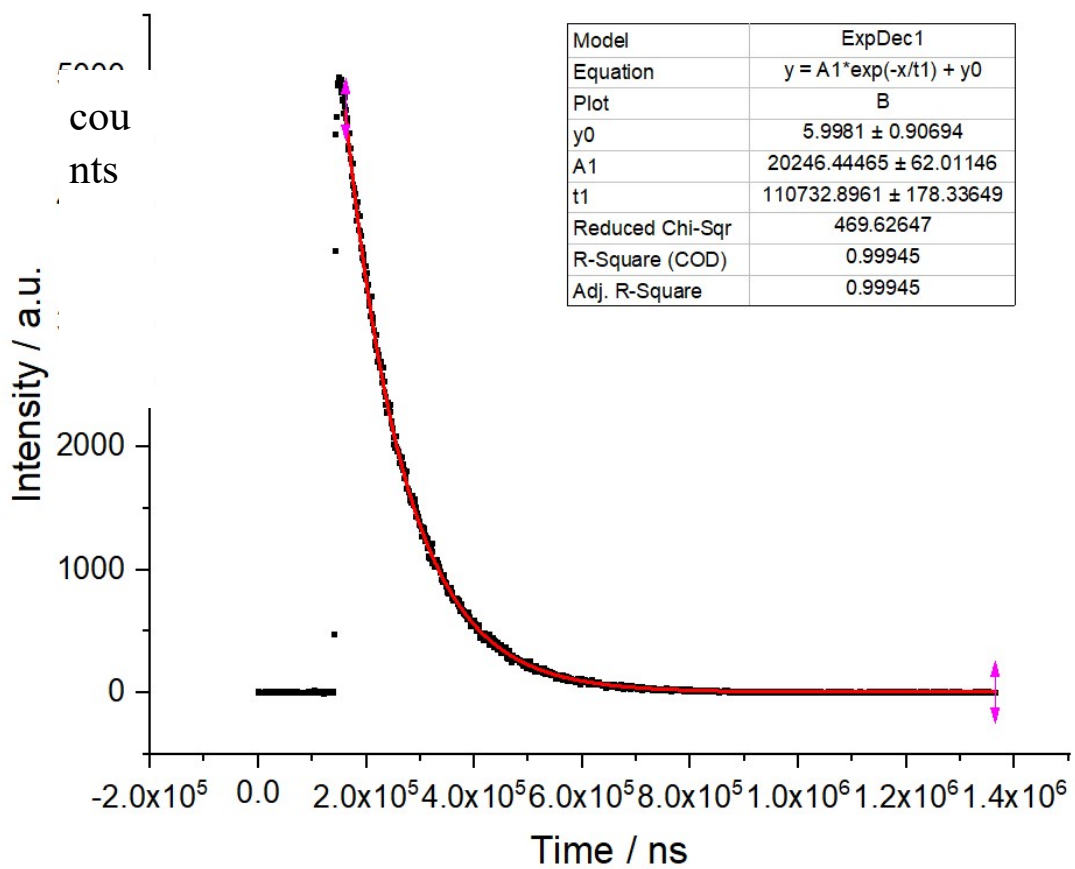


Figure S13. Excited state lifetime and the best fit of the experimental data for the $[\text{Cr}(\text{Mebipzp})_2]^{3+}$ complex ($\lambda_{\text{exc}} = 480$ nm) in aerated acetonitrile solution

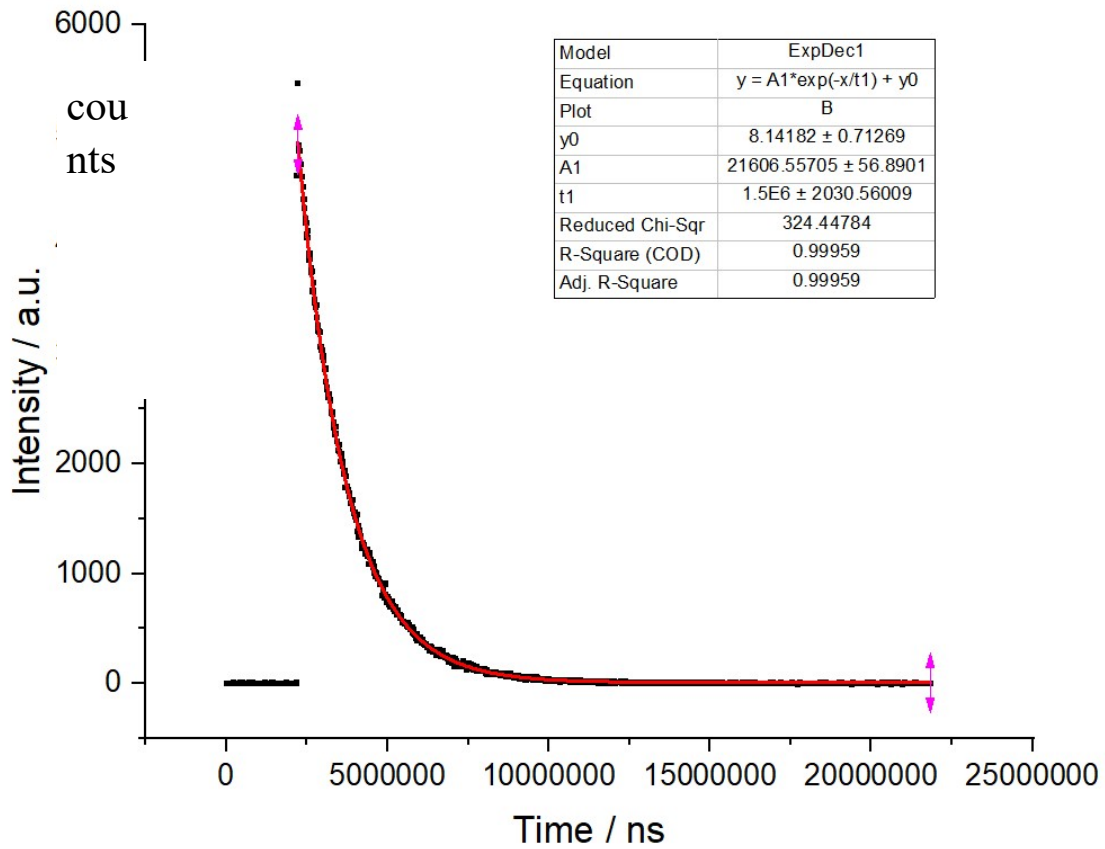


Figure S14. Excited state lifetime and the best fit of the experimental data for the $[\text{Cr}(\text{Mebipzp})_2]^{3+}$ complex ($\lambda_{\text{exc}} = 480$ nm) at 77 K in frozen acetonitrile

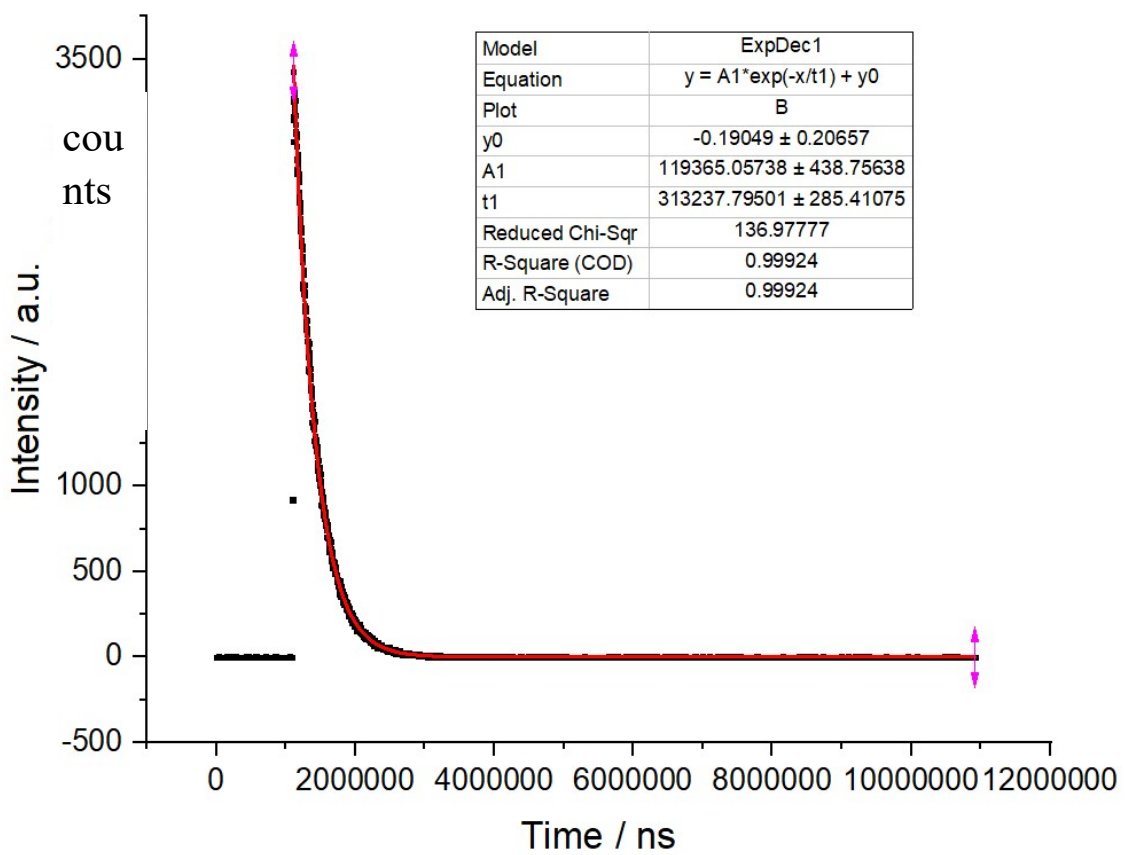


Figure S15. Excited state lifetime and the best fit of the experimental data for the $[\text{Cr}(\text{IMEbipzp})_2]^{3+}$ complex ($\lambda_{\text{exc}} = 480$ nm) in deaerated acetonitrile solution

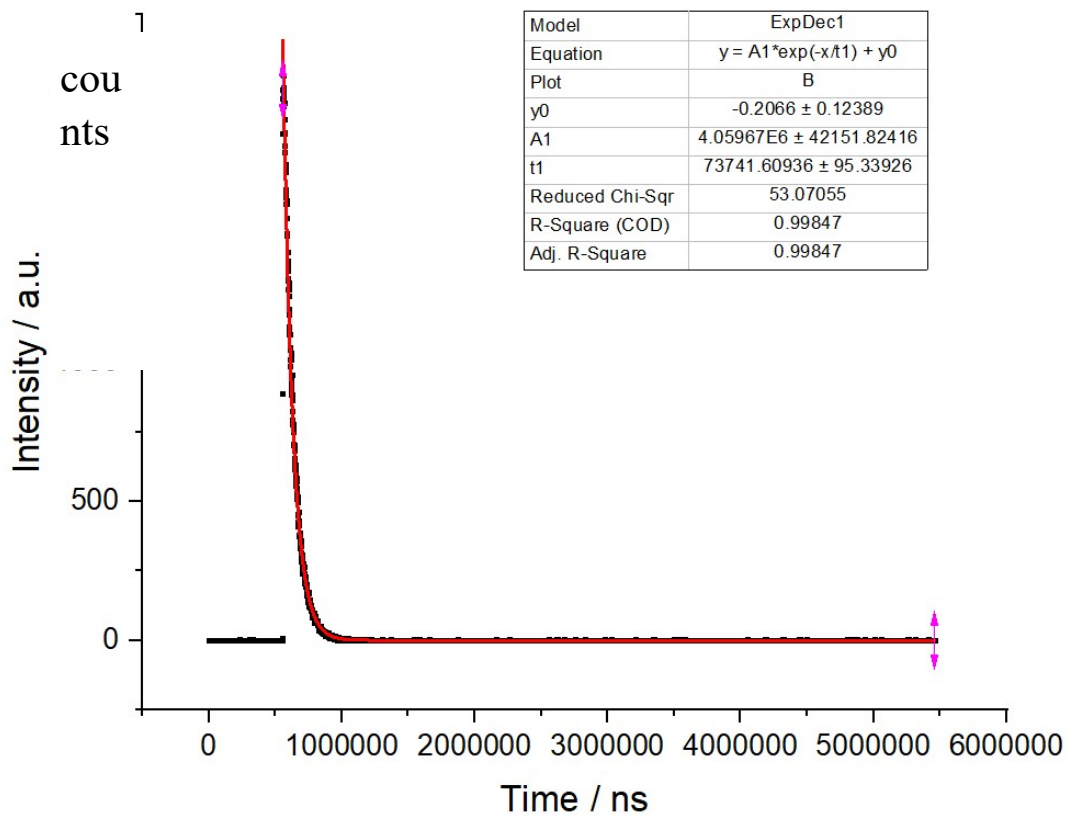


Figure S16. Excited state lifetime and the best fit of the experimental data for the $[\text{Cr}(\text{IMEbipzp})_2]^{3+}$ complex ($\lambda_{\text{exc}} = 480$ nm) in aerated acetonitrile solution.

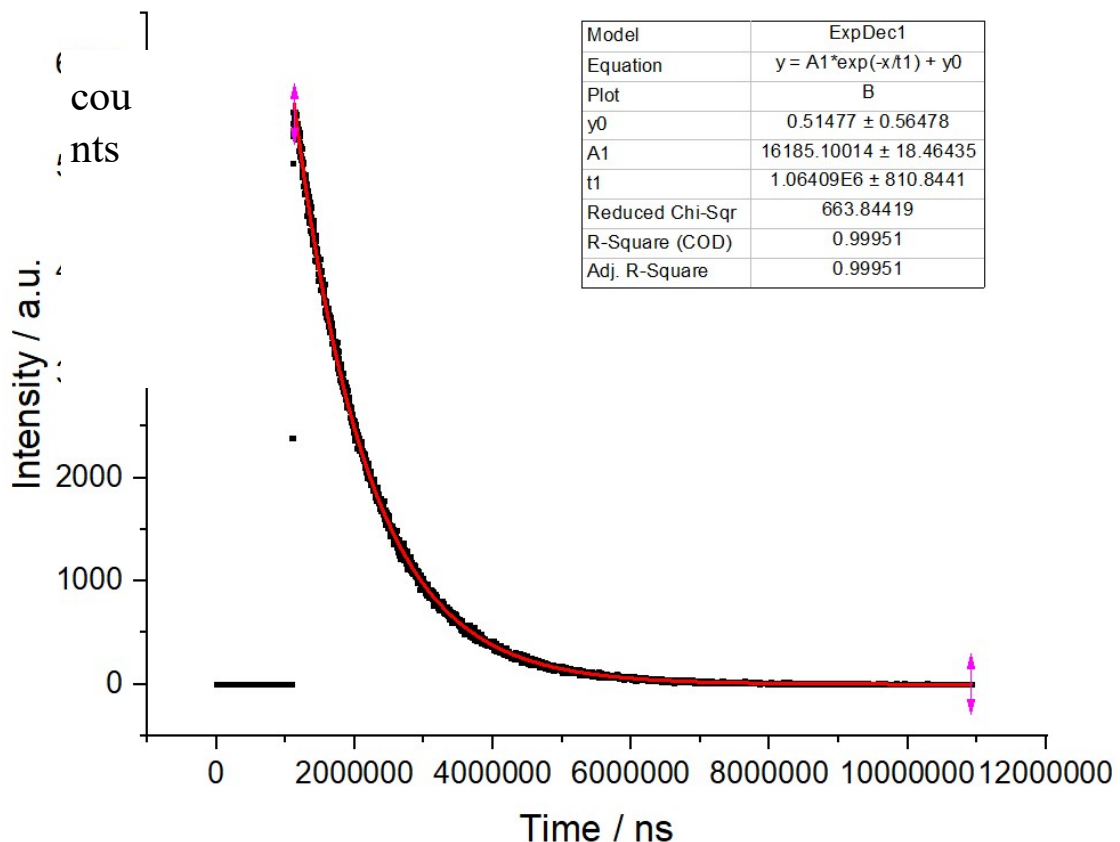


Figure S17. Excited state lifetime and the best fit of the experimental data for the $[\text{Cr}(\text{IMEbipzp})_2]^{3+}$ complex ($\lambda_{\text{exc}} = 480$ nm) at 77 K in frozen acetonitrile.

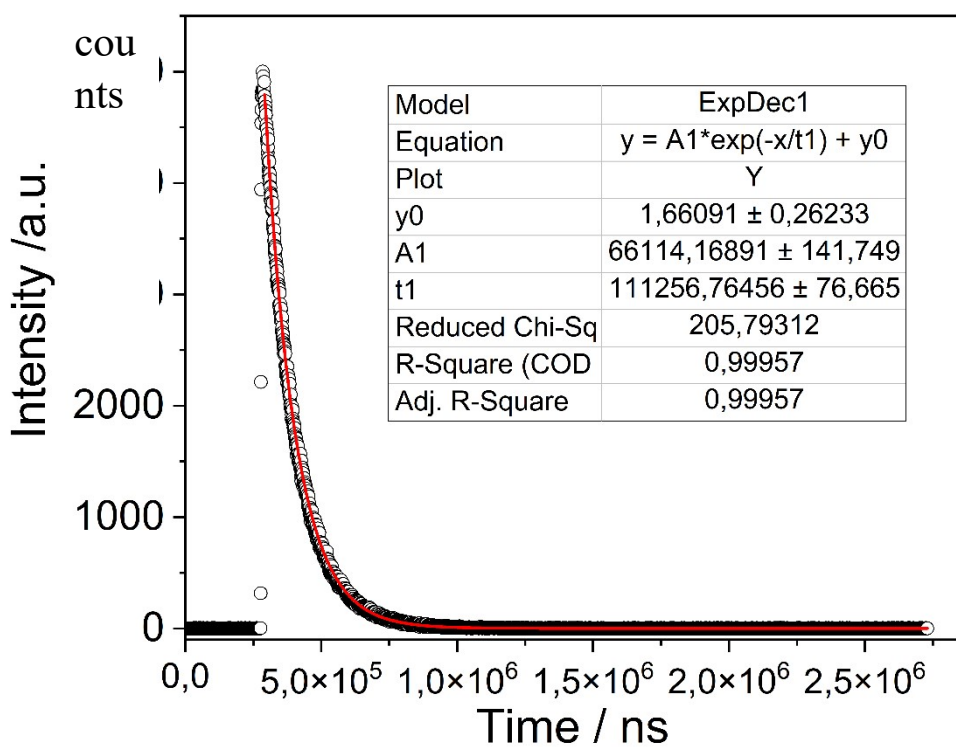


Figure S18. Excited state lifetime and the best fit of the experimental data for the $[\text{Cr}(\text{bip}^*)_2]^{3+}$ complex ($\lambda_{\text{exc}} = 450$ nm) in deaerated acetonitrile solution at room temperature.

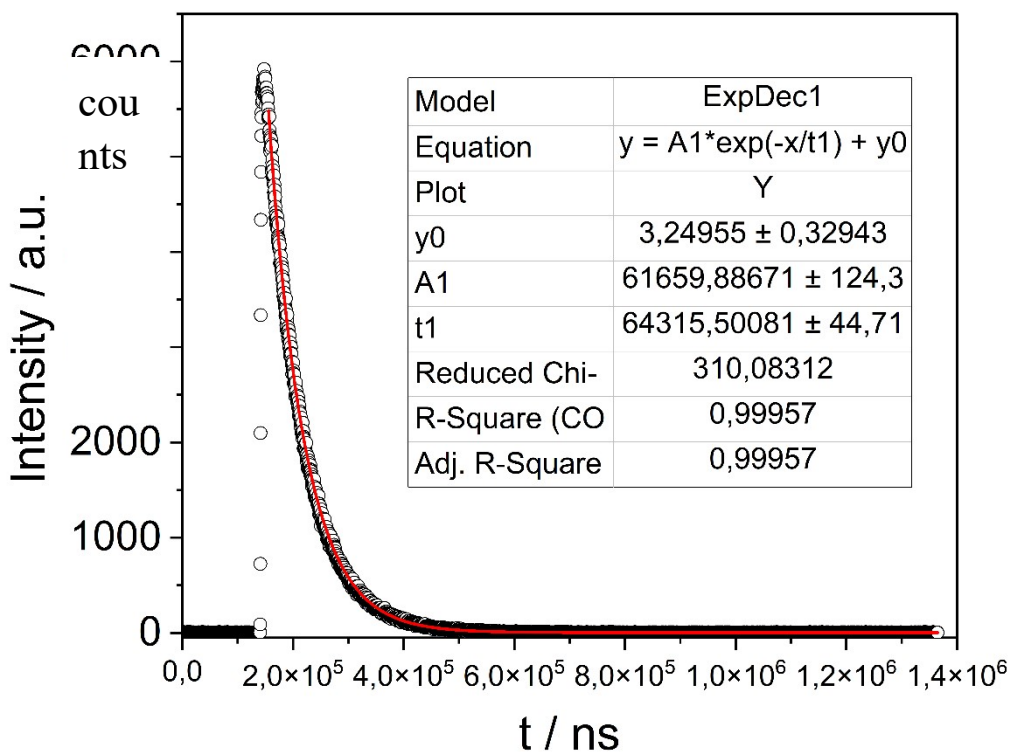


Figure S19. Excited state lifetime and the best fit of the experimental data for the $[\text{Cr}(\text{bip}^*)_2]^{3+}$ complex ($\lambda_{\text{exc}} = 450$ nm) in aerated acetonitrile solution at room temperature.

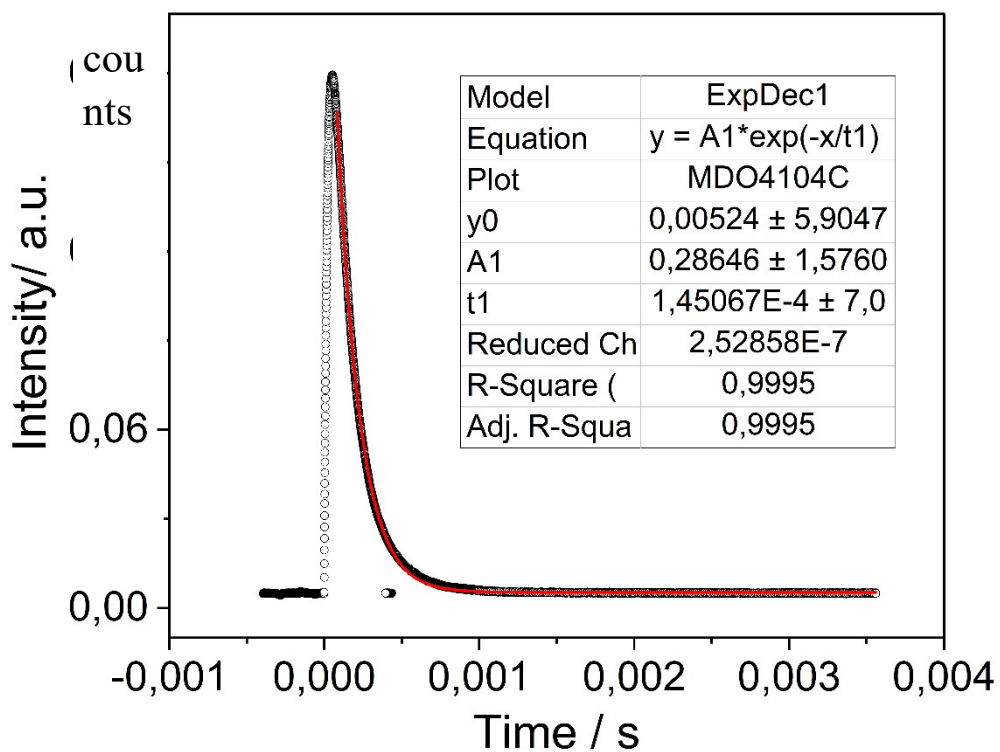


Figure S20. Excited state lifetime and the best fit of the experimental data for the $[\text{Cr}(\text{bip}^*)]^{3+}$ complex ($\lambda_{\text{exc}} = 450 \text{ nm}$) at 77 K in frozen acetonitrile.

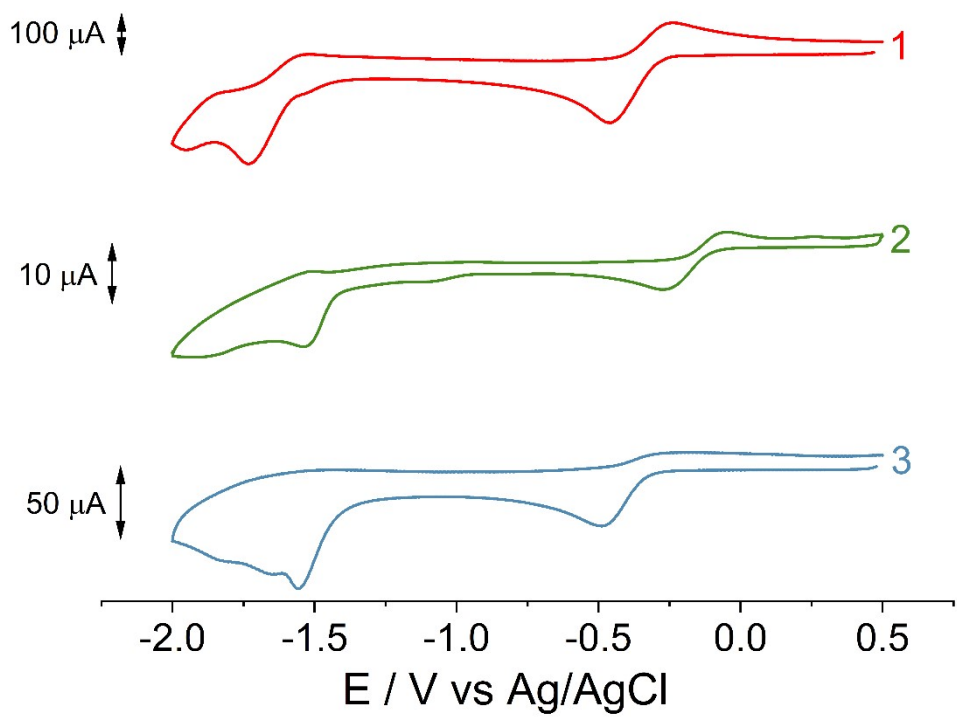


Figure S21. CV diagrams of 1 – 3 in CH_3CN containing 0.1 M TBAPF₆.

Theoretical studies

The Orca^[S3] (version 5.0.3) and Gaussian 16^[S4] (revision A.03) software packages were used to investigate the structural and electronic properties of the studied complexes. Starting from the X-ray diffraction structures, the ground, 4A_2 state, structure of the two complexes were obtained from DFT optimizations using the unrestricted version of the Becke three-parameters exchange function in combination with the Lee-Yang-Parr correlation functional (UB3LYP). The Ahlrichs' polarized valence triple- ζ basis set def2-TZVPP was used for these optimizations. The D3 version of Grimme's dispersion with Becke-Johnson damping (GD3BJ) was applied. Solvent effects were included via the Conductor-like Polarizable Continuum Model (CPCM) as implemented in Orca 5.0.3 with the dielectric constant of acetonitrile. Optimized geometries were confirmed to be stationary points by analysis of their vibrational frequencies. Tight convergence criteria were selected for the optimization step. The resolution of identity approach for the Coulomb term in combination with the chain-of-spheres approximation for the exchange term (RIJCOSX) was applied. The zero-order relativistic approximation (ZORA) was used to describe relativistic effects. Spin density information was extracted from the optimized geometries.

Ab initio ligand field (AILF) analysis was performed over the optimized geometries using Orca version 5.0.3. The complete-active-space self-consistent field method (CASSCF) together with the fully internally contracted N-electron valence perturbation theory to second order (FIC-NEVPT2) was used, selecting only the 3d orbitals as active space (CASSCF(3,5)/FIC-NEVPT2) and using the def2-TZVPP basis set in combination with the RI-JK approximation (def2/JK as auxiliary base). 10 quartet and 40 doublet roots were computed for the AILF analysis.

To accurately model the ligand field, CASSCF together with FIC-NEVPT2 was used. Dominant bonding/antibonding orbitals formed between ligand and chromium and a second d shell were considered, creating an active space of 7 electrons and 12 orbitals (CASSCF(7,12)/FIC-NEVPT2). 10 quartet and 9 doublet roots were computed to calculate the energies of the excited states.

The 50 lowest energetic transitions were calculated by TD-DFT as implemented in Gaussian 16, using the unrestricted version of the Coulomb-attenuated B3LYP functional (UCAM-B3LYP), selecting the def2-TZVPP basis set and considering solvent effects. Electronic transitions were corrected by -0.3 eV to better fit experimental results. Charge transfer numbers were computed using TheoDORE 2.4.^[S5] Electron density difference maps (EDDMs) were obtained using GaussSum,^[S6] and visualized using UCSF Chimera (isoval=0.002).^[S7]

Optimized Geometries

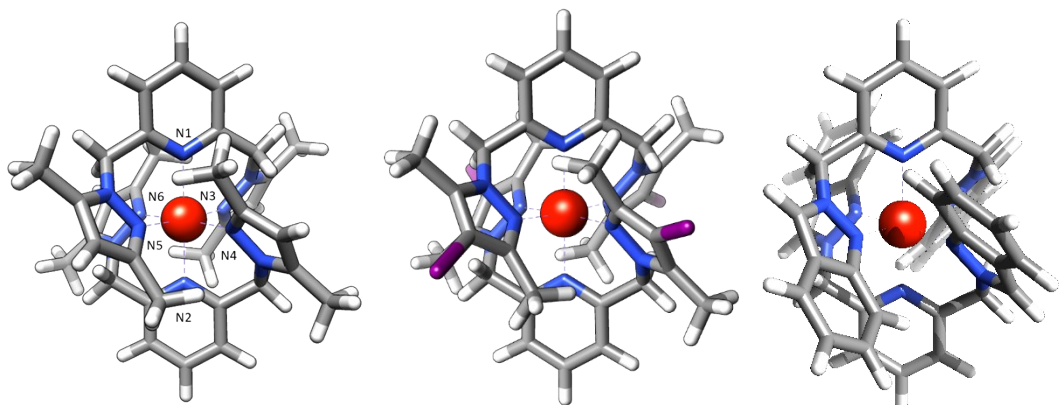


Figure S22. DFT optimized geometries of the quartet ground state of **1**(left), **2** (middle) and **3** (right). Spin density at the Cr center: 3.162171, 3.143759 and 3.111739 (respectively).

Table S6. Bond lengths (\AA) and angles ($^\circ$) of **1** and **2** from XRD measurements and DFT calculations. and CASSCF(7,12)/FIC-NEVPT2 results of **1**, **2** and **3**. Energies in cm^{-1} .

	3		2		1	
	XRD	DFT	XRD	DFT	XRD	DFT
Cr–N1	2.0777	2.1313	2.1040	2.1169	2.0868	2.1137
Cr–N2	2.0976	2.1314	2.0910	2.1168	2.0812	2.1136
Cr–N3	1.9976	2.0572	2.0687	2.0819	2.0471	2.0764
Cr–N4	2.0433	2.0564	2.0656	2.0788	2.0634	2.0765
Cr–N5	2.0293	2.0564	2.0650	2.0837	2.0550	2.0765
Cr–N6	2.0470	2.0572	2.0677	2.0802	2.0527	2.0764
N1–Cr–N2	178.48	179.84	178.97	179.96	177.28	179.99
N1–Cr–N3	92.93	87.14	87.60	87.72	87.97	88.24
N1–Cr–N4	88.83	92.67	91.98	92.20	90.20	91.75
N1–Cr–N5	91.69	87.22	88.24	87.92	88.44	88.24
N1–Cr–N6	88.52	92.97	92.70	92.29	93.39	91.76
N2–Cr–N3	87.31	92.97	91.37	92.32	90.36	91.75
N2–Cr–N4	92.65	87.21	88.03	87.81	87.82	88.25
N2–Cr–N5	88.07	92.67	92.79	92.04	93.29	91.77
N2–Cr–N6	90.00	87.15	87.30	87.70	88.63	88.24
N3–Cr–N4	94.41	94.20	94.32	93.64	95.43	93.72
N3–Cr–N5	175.38	174.36	175.83	175.65	176.10	176.48
N3–Cr–N6	85.15	86.05	86.55	86.48	85.80	86.39
N4–Cr–N5	85.65	86.10	85.98	86.50	86.11	86.40
N4–Cr–N6	177.29	174.36	175.27	175.51	176.25	176.49
N5–Cr–N6	95.00	94.20	93.49	93.72	92.89	93.70

	^2E (1)	^2E (2)	$^2\text{T}_1$ (1)	$^2\text{T}_1$ (2)	$^2\text{T}_1$ (3)	$^2\text{T}_2$ (1)	$^2\text{T}_2$ (2)	$^2\text{T}_2$ (3)	$^4\text{T}_2$ (1)	$^4\text{T}_2$ (2)	$^4\text{T}_2$ (3)
1	15557	16110	15247	15314	16019	23553	23700	23976	21386	21410	22690
2	15558	16104	15230	15377	16033	23490	23699	23924	21205	21244	22522
3	15342	15916	14741	14933	15722	23268	23410	23909	20486	21446	22129

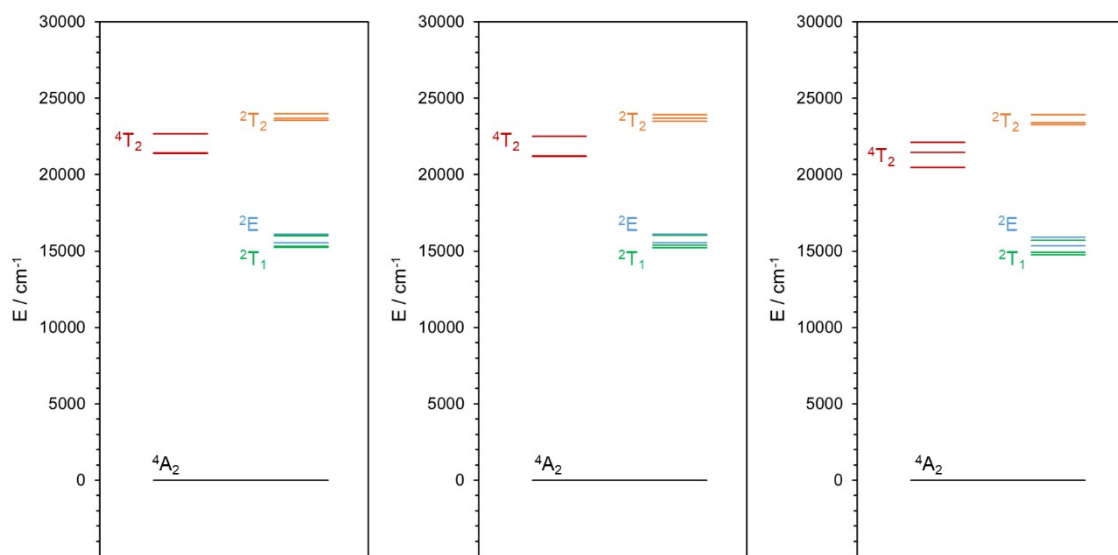


Figure S23. Schematic representation of the energy levels for the calculated (CASSCF(7,12)/FIC-NEVPT2) excited states of **1** (left), **2** (middle) and **3** (right).

Table S7. Orbitals used in the CASSCF(7,12)/FIC-NEVPT2 calculations for **1** (isoval=0.04).

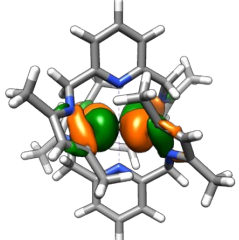
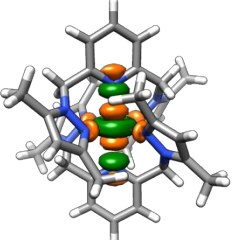
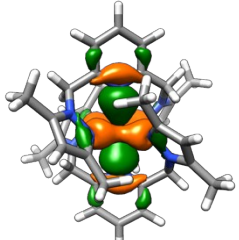
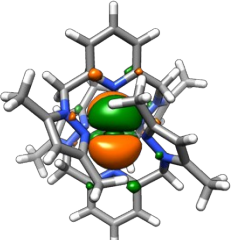
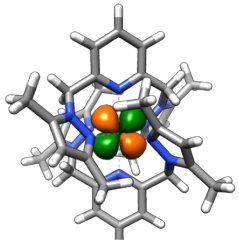
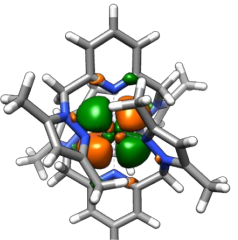
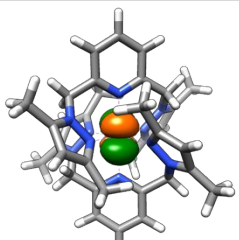
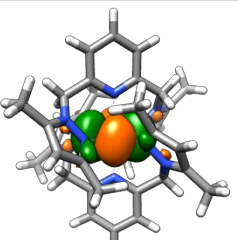
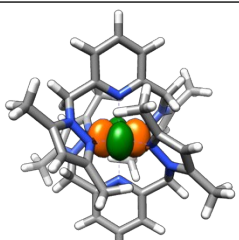
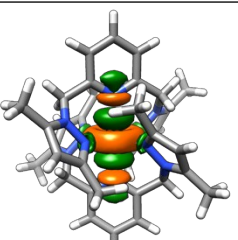
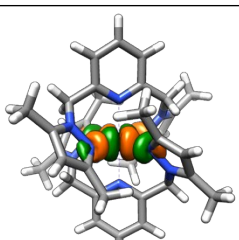
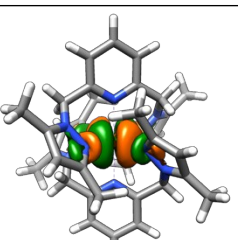
#	E (hartrees)	Orbital	#	Energy	Orbital
165	-0.877399		171	-0.205190	
166	-0.867665		172	0.730059	
167	-0.421046		173	0.753275	
168	-0.411074		174	0.755171	
169	-0.403576		175	1.365514	
170	-0.199660		176	1.405373	

Table S8. Orbitals used in the CASSCF(7,12)/FIC-NEVPT2 calculations for **2** (isoval=0.04).

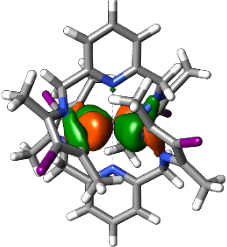
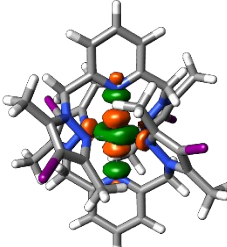
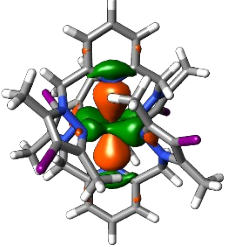
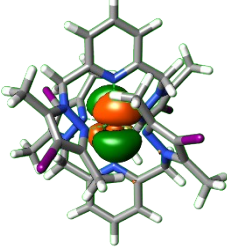
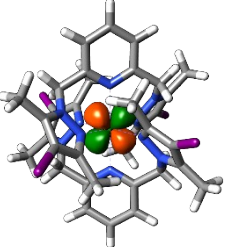
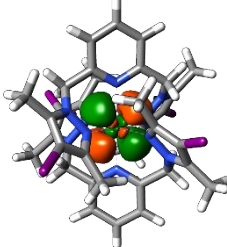
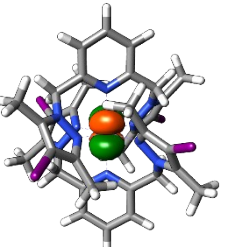
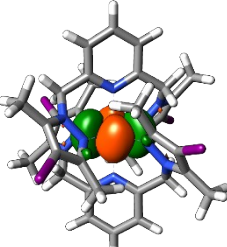
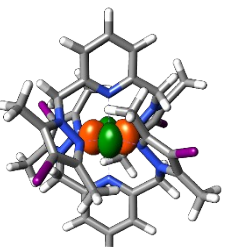
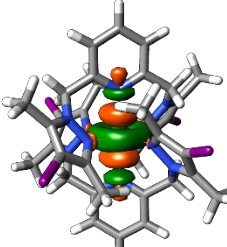
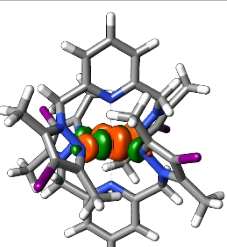
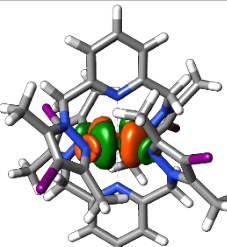
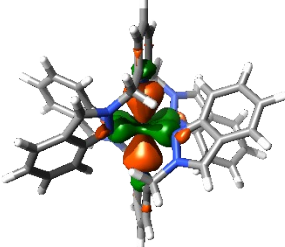
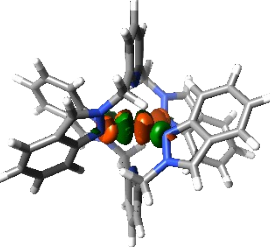
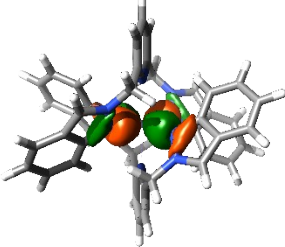
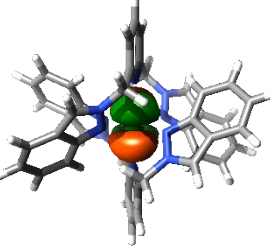
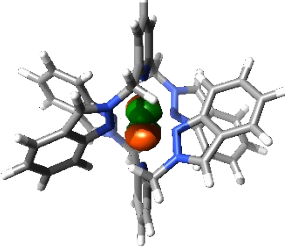
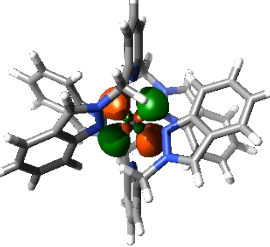
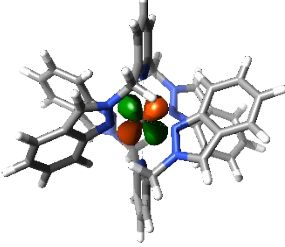
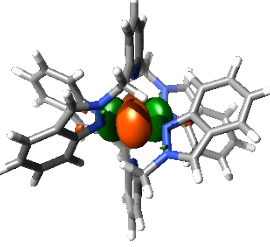
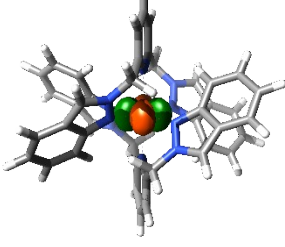
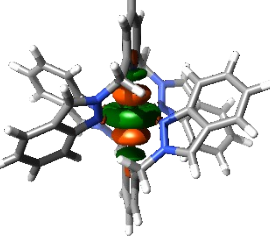
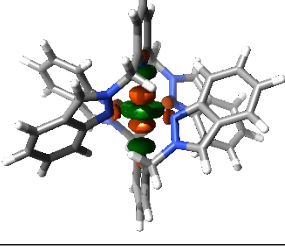
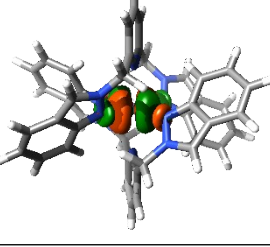
#	E (hartrees)	Orbital	#	Energy	Orbital
213	-0.876005		219	-0.209919	
214	-0.868147		220	0.728399	
215	-0.424772		221	0.750394	
216	-0.414683		222	0.749667	
217	-0.408243		223	1.356002	
218	-0.205755		224	1.387980	

Table S9. Orbitals used in the CASSCF(7,12)/FIC-NEVPT2 calculations for **3** (isoval=0.04).

#	Energy (Hartrees)	Orbital	#	Energy (Hartrees)	Orbital
185	-0.856996		191	-0.180911	
186	-0.871802		192	0.758509	
187	-0.407756		193	0.741001	
188	-0.396342		194	0.771543	
189	-0.389943		195	1.355980	
190	-0.195714		196	1.427039	

Electronic transitions

Table S10. Calculated 100 lowest electronic transitions for compound **1**, their energies (in nm) and oscillatory strength (in cgs units).

Transition number	Wavelength / nm	Osc. Strength / cgs	Transition number	Wavelength / nm	Osc. Strength / cgs
1	460.7	0.000081863	41	282.9	0.000889228
2	448.7	0.000259487	42	282.5	0.000001299
3	425.0	0.000862935	43	282.3	0.003932199
4	407.0	0.000000016	44	281.3	0.020161778
5	363.2	0.001127841	45	280.8	0.011463406
6	361.3	0.027948874	46	280.6	0.005825521
7	348.1	0.000892393	47	279.8	0.001363765
8	343.5	0.001190661	48	277.5	0.000000091
9	336.5	0.005098185	49	276.6	0.013389699
10	336.3	0.000031111	50	276.2	0.000003607
11	336.2	0.005176938	51	274.6	0.000279987
12	335.7	0.000647932	52	274.3	0.010322406
13	333.6	0.013829627	53	274.3	0.000059324
14	324.5	0.003391283	54	273.5	0.000000048
15	323.0	0.000000132	55	272.4	0.000259427
16	319.1	0.002116681	56	272.1	0.002594494
17	317.6	0.003542893	57	271.4	0.002749908
18	317.3	0.018891410	58	270.3	0.000273288
19	316.1	0.000000628	59	269.9	0.002898735
20	314.2	0.012021121	60	269.3	0.001554501
21	314.1	0.046859758	61	269.0	0.000000184
22	311.3	0.000650194	62	268.2	0.009999719
23	310.2	0.003400632	63	267.9	0.000057385
24	308.1	0.000001021	64	267.8	0.005520642
25	306.8	0.020748280	65	266.5	0.002296036
26	306.4	0.010516683	66	265.6	0.000000645
27	305.2	0.009946552	67	265.0	0.001347851
28	304.9	0.040115754	68	264.6	0.027537825
29	303.1	0.000000020	69	264.2	0.000065921
30	299.7	0.000435332	70	264.2	0.016717507
31	297.4	0.000000526	71	264.0	0.000027847
32	294.8	0.004628151	72	263.6	0.000074037
33	290.9	0.000381853	73	263.4	0.000129992
34	290.5	0.003349217	74	263.2	0.006593176
35	289.6	0.000000011	75	262.1	0.013083716
36	286.1	0.002487443	76	261.9	0.000908007
37	286.1	0.000000104	77	261.6	0.000000686
38	285.4	0.005353684	78	261.2	0.002838866
39	284.7	0.004214731	79	259.2	0.000000491
40	284.0	0.007086297	80	257.0	0.009056044

Transition number	Wavelength / nm	Osc. Strength / cgs	Transition number	Wavelength / nm	Osc. Strength / cgs
81	257.0	0.011461363	91	243.5	0.000600390
82	255.2	0.004128707	92	242.9	0.003617675
83	254.6	0.000000128	93	240.0	0.000758261
84	253.2	0.003872623	94	239.9	0.000000715
85	251.8	0.000000031	95	239.4	0.000397302
86	251.5	0.006550820	96	239.2	0.000000018
87	251.1	0.007999773	97	238.9	0.022079010
88	250.6	0.000770306	98	238.5	0.000542087
89	250.2	0.001993544	99	238.4	0.000000170
90	250.2	0.000038909	100	238.1	0.008775422

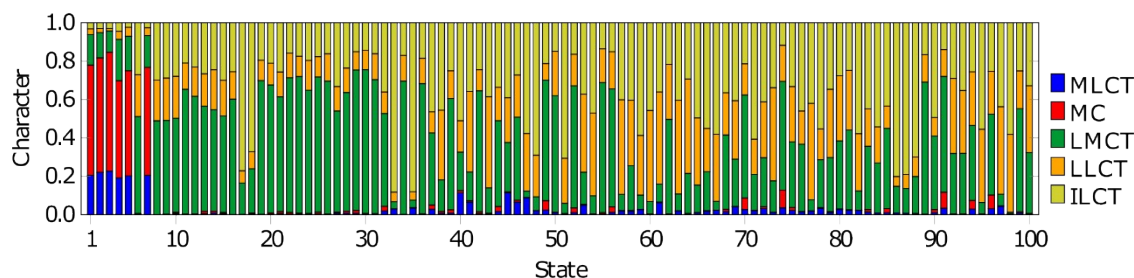


Figure S24. TD-DFT charge transfer numbers of **1** defined from 0 to 1 of the first 50 electronic transitions.

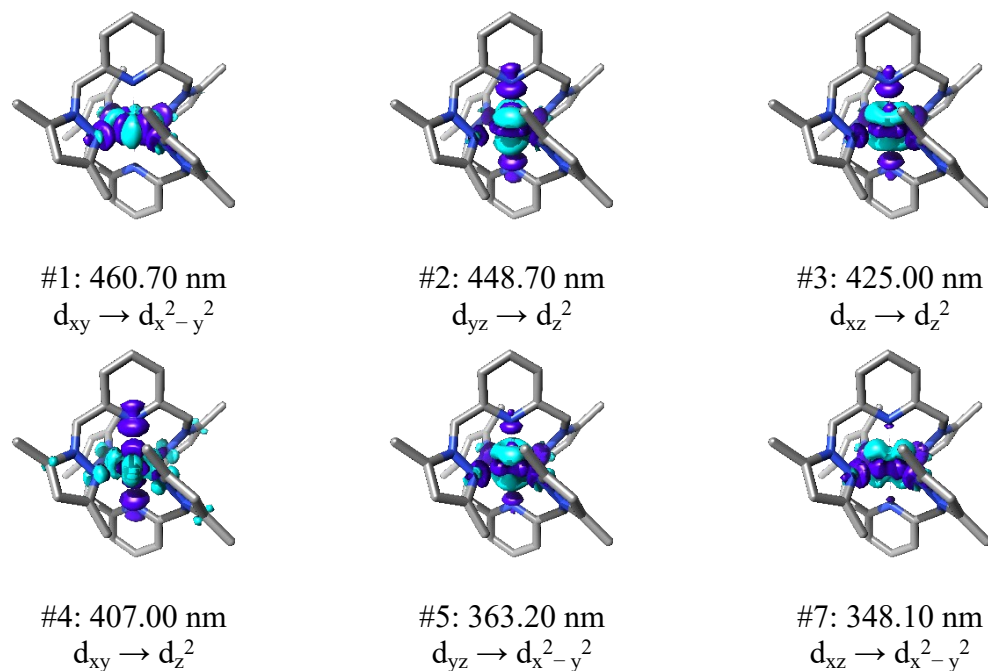


Figure S25. Electron density difference maps (EDDM) of the six MC electronic transitions calculated for **1** (isoval 0.002). Blue: density loss; Purple: density gain.

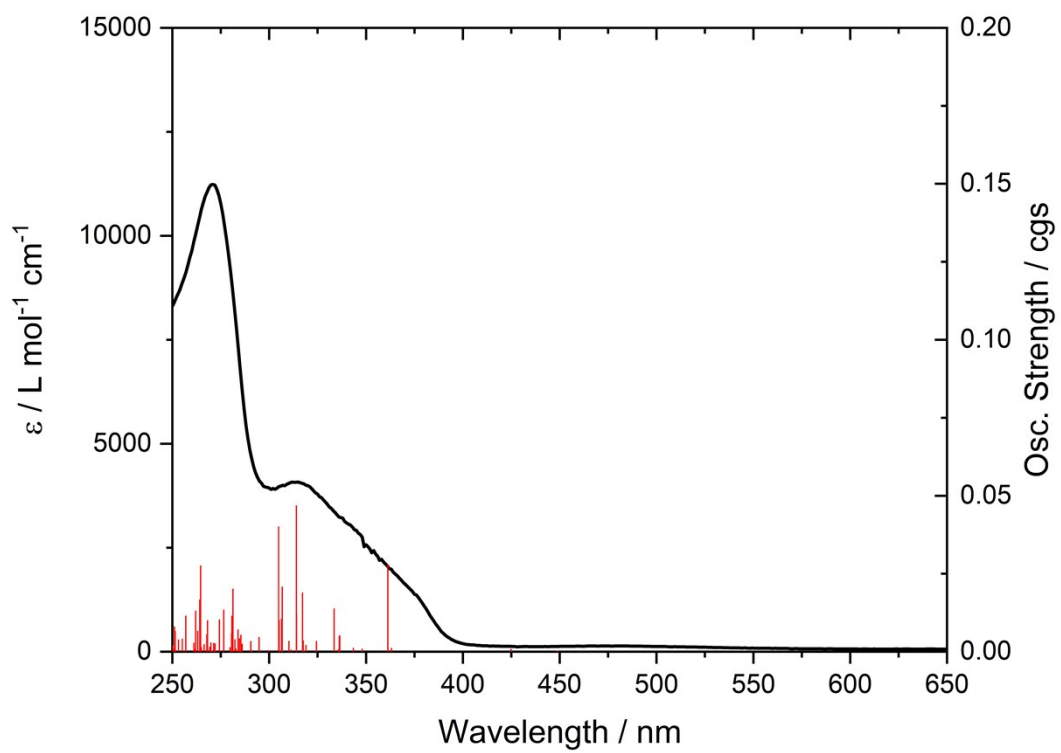


Figure S26. Experimental UV-Vis spectrum of compound **1** in acetonitrile and calculated oscillatory strength of the calculated electronic transitions.

Table S7. Calculated 100 lowest electronic transitions for compound **2**, their energies (in nm) and oscillatory strength (in cgs units).

Transition number	Wavelength / nm	Osc. Strength / cgs	Transition number	Wavelength / nm	Osc. Strength / cgs
1	473.10	0.000108964	41	318.20	0.000263198
2	456.50	0.000452785	42	316.90	0.008250000
3	433.60	0.002120000	43	316.30	0.058120000
4	421.70	0.016060000	44	315.80	0.000985345
5	418.80	0.000068200	45	315.10	0.000107209
6	418.20	0.001340000	46	314.90	0.000030102
7	417.20	0.000016529	47	314.80	0.000192036
8	412.10	0.016820000	48	314.10	0.000598102
9	393.00	0.004440000	49	313.70	0.000030902
10	391.50	0.035680000	50	313.30	0.000015566
11	390.50	0.028460000	51	313.20	0.000275754
12	385.40	0.001030000	52	312.20	0.031220000
13	384.30	0.000661078	53	310.60	0.000008509
14	383.20	0.000032186	54	309.30	0.000037478
15	381.90	0.000000908	55	306.80	0.000039574
16	381.10	0.001170000	56	306.70	0.000757662
17	377.20	0.006460000	57	306.60	0.000260772
18	368.10	0.000055521	58	306.20	0.001170000
19	361.70	0.038660000	59	305.60	0.000515571
20	359.20	0.001340000	60	301.60	0.000104348
21	354.00	0.000060078	61	301.40	0.000234251
22	353.70	0.001060000	62	301.10	0.000031909
23	352.50	0.000393966	63	300.80	0.000012235
24	344.60	0.000040619	64	300.10	0.000014117
25	339.60	0.013930000	65	300.00	0.000349261
26	338.40	0.000355893	66	299.80	0.000059690
27	338.10	0.000377016	67	299.50	0.000052418
28	336.00	0.000003415	68	296.90	0.003600000
29	334.50	0.000046120	69	293.00	0.000007392
30	330.80	0.000196906	70	291.60	0.000393282
31	326.80	0.006340000	71	290.50	0.000752906
32	326.30	0.000424654	72	289.90	0.000006983
33	325.00	0.008490000	73	289.60	0.000008326
34	323.10	0.000030904	74	289.10	0.001010000
35	322.90	0.002350000	75	287.70	0.000320723
36	322.00	0.002180000	76	287.00	0.000187108
37	321.30	0.000376841	77	285.60	0.017430000
38	319.40	0.001310000	78	284.90	0.017870000
39	318.60	0.000213804	79	284.10	0.019970000
40	318.40	0.000317286	80	283.30	0.005930000

Transition number	Wavelength / nm	Osc. Strength / cgs	Transition number	Wavelength / nm	Osc. Strength / cgs
81	283.00	0.000121244	91	277.10	0.000200959
82	282.90	0.000757880	92	277.10	0.000194927
83	282.90	0.000597674	93	276.70	0.003830000
84	282.50	0.000952859	94	276.40	0.010510000
85	282.30	0.000178893	95	275.60	0.001890000
86	282.30	0.001010000	96	275.40	0.002880000
87	278.60	0.011260000	97	275.30	0.001330000
88	278.30	0.000042284	98	274.60	0.001930000
89	278.00	0.001410000	99	273.80	0.009130000
90	277.80	0.000243845	100	269.70	0.031430000

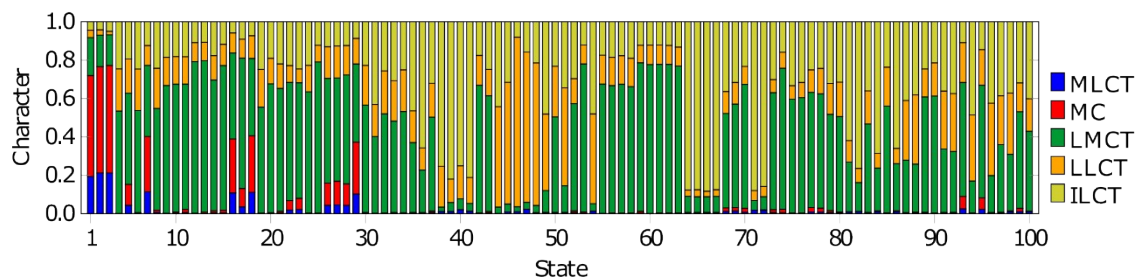


Figure S27. TD-DFT charge transfer numbers of **2** defined from 0 to 1 of the first 100 electronic transitions.

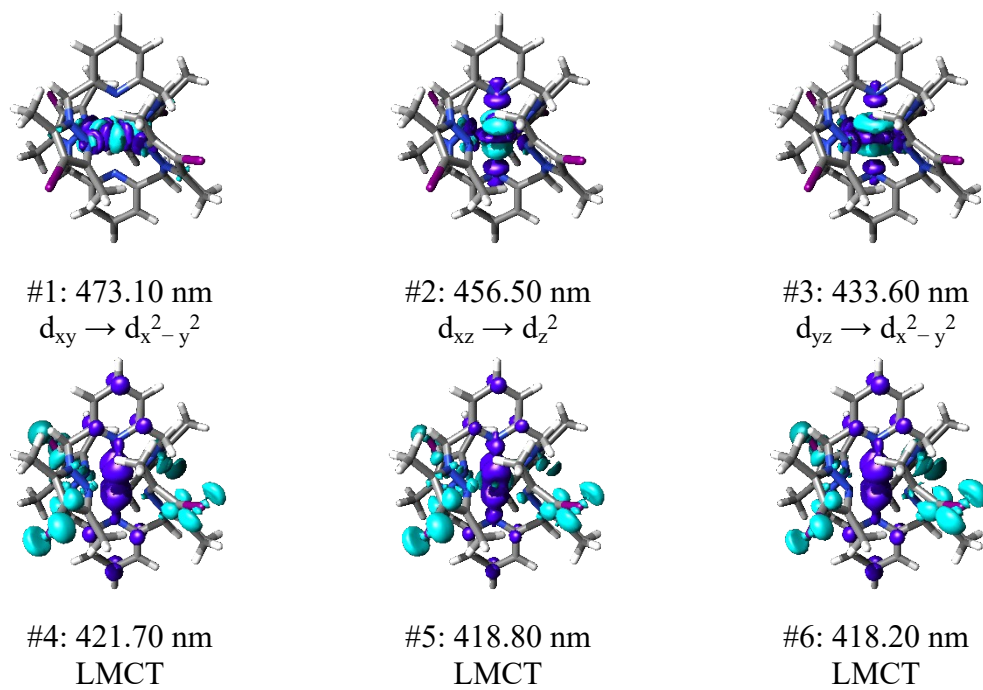


Figure S28. Electron density difference maps (EDDM) of the first six electronic transitions calculated for **2** (isoval 0.002). Blue: density loss; Purple: density gain.

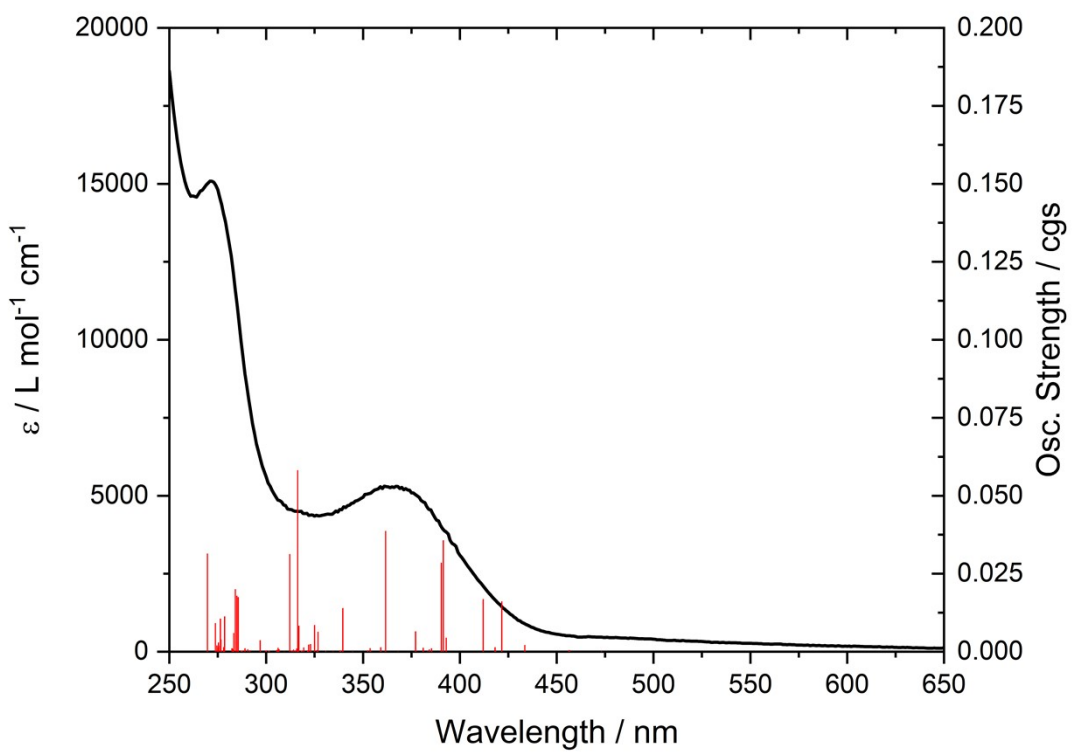


Figure S29. Experimental UV-Vis spectrum of compound **2** in acetonitrile and calculated oscillatory strength of the calculated electronic transitions. a) Full view; b) Zoom view.

Table S7. Calculated 100 lowest electronic transitions for compound **3**, their energies (in nm) and oscillatory strength (in cgs units).

Transition number	Wavelength / nm	Osc. Strength / cgs	Transition number	Wavelength / nm	Osc. Strength / cgs
1	480.90	0.000502828	41	327.40	0.000419571
2	469.50	0.000072148	42	324.10	0.000002021
3	452.60	0.000002317	43	322.10	0.000448382
4	449.10	0.042220000	44	321.10	0.000000117
5	443.40	0.034090000	45	320.20	0.010290000
6	438.00	0.001590000	46	315.20	0.005560000
7	424.10	0.000000218	47	312.70	0.002310000
8	423.60	0.019750000	48	311.50	0.000901356
9	418.40	0.000014488	49	309.80	0.000005275
10	414.30	0.010280000	50	309.20	0.000060072
11	404.00	0.000000630	51	306.60	0.002170000
12	398.80	0.000001024	52	306.30	0.002850000
13	394.80	0.006230000	53	305.70	0.000376664
14	385.70	0.000451373	54	305.10	0.000948934
15	384.80	0.000019833	55	304.80	0.000618534
16	383.60	0.011100000	56	304.20	0.011410000
17	376.20	0.001330000	57	299.00	0.000338436
18	375.60	0.097690000	58	297.70	0.000262351
19	373.30	0.073920000	59	297.50	0.009260000
20	363.50	0.088430000	60	297.00	0.052430000
21	360.70	0.005600000	61	296.70	0.001060000
22	359.80	0.001540000	62	295.50	0.001140000
23	353.50	0.000003055	63	295.40	0.000032476
24	347.20	0.014470000	64	294.60	0.000262728
25	345.40	0.004540000	65	294.40	0.000066425
26	341.80	0.000007731	66	294.30	0.000439374
27	341.20	0.003760000	67	294.20	0.000348638
28	340.30	0.001190000	68	293.80	0.000009963
29	338.70	0.000026103	69	293.20	0.003590000
30	337.40	0.000305482	70	291.50	0.000000426
31	336.60	0.000129417	71	291.00	0.000000251
32	334.70	0.004950000	72	291.00	0.004640000
33	334.20	0.001630000	73	290.50	0.004660000
34	334.20	0.000095017	74	289.40	0.000539907
35	332.40	0.015170000	75	289.30	0.000158726
36	331.20	0.000176195	76	289.30	0.000105146
37	330.70	0.001130000	77	289.10	0.000002374
38	330.40	0.000588991	78	288.70	0.001650000
39	329.40	0.001860000	79	288.20	0.003640000
40	327.50	0.002100000	80	286.50	0.003540000

Transition number	Wavelength / nm	Osc. Strength / cgs	Transition number	Wavelength / nm	Osc. Strength / cgs
81	286.20	0.004070000	91	280.50	0.074520000
82	285.80	0.000378163	92	278.10	0.004930000
83	283.90	0.000553583	93	277.80	0.003430000
84	283.70	0.010230000	94	276.40	0.000233219
85	283.30	0.004560000	95	276.20	0.000844896
86	282.90	0.000234102	96	275.60	0.000359979
87	281.90	0.006860000	97	275.30	0.000024417
88	280.90	0.000001937	98	274.40	0.000685888
89	280.70	0.070110000	99	274.40	0.014700000
90	280.50	0.034560000	100	273.90	0.000135663

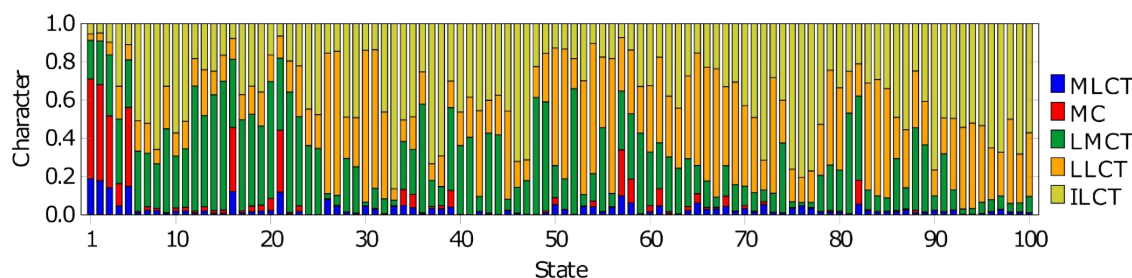


Figure S30. TD-DFT charge transfer numbers of **3** defined from 0 to 1 of the first 100 electronic transitions.

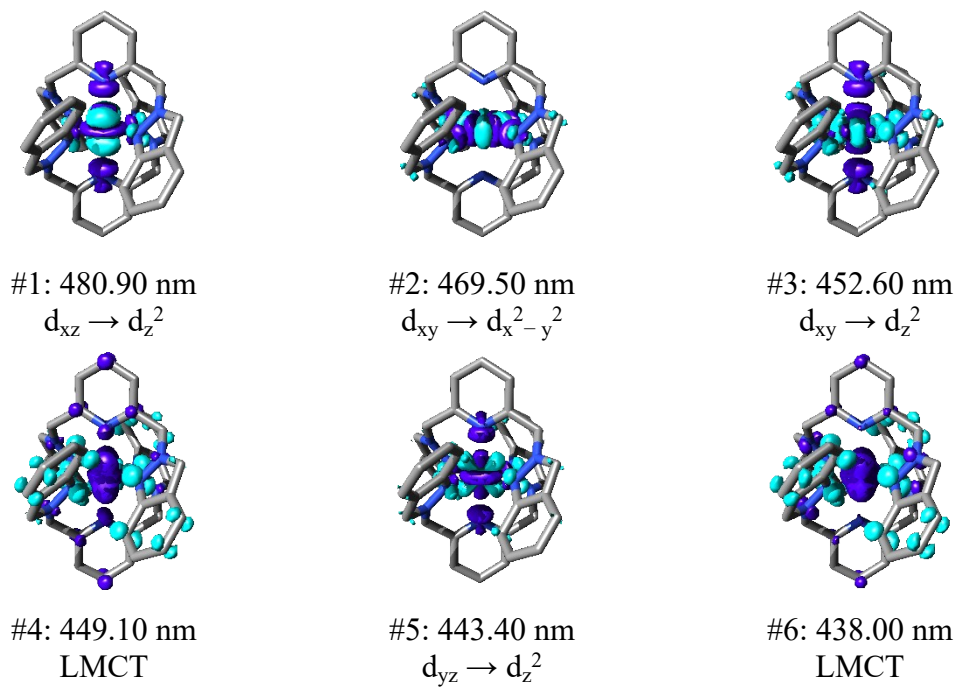


Figure S31. Electron density difference maps (EDDM) of the first six electronic transitions calculated for **3** (isoval 0.002). Blue: density loss; Purple: density gain.

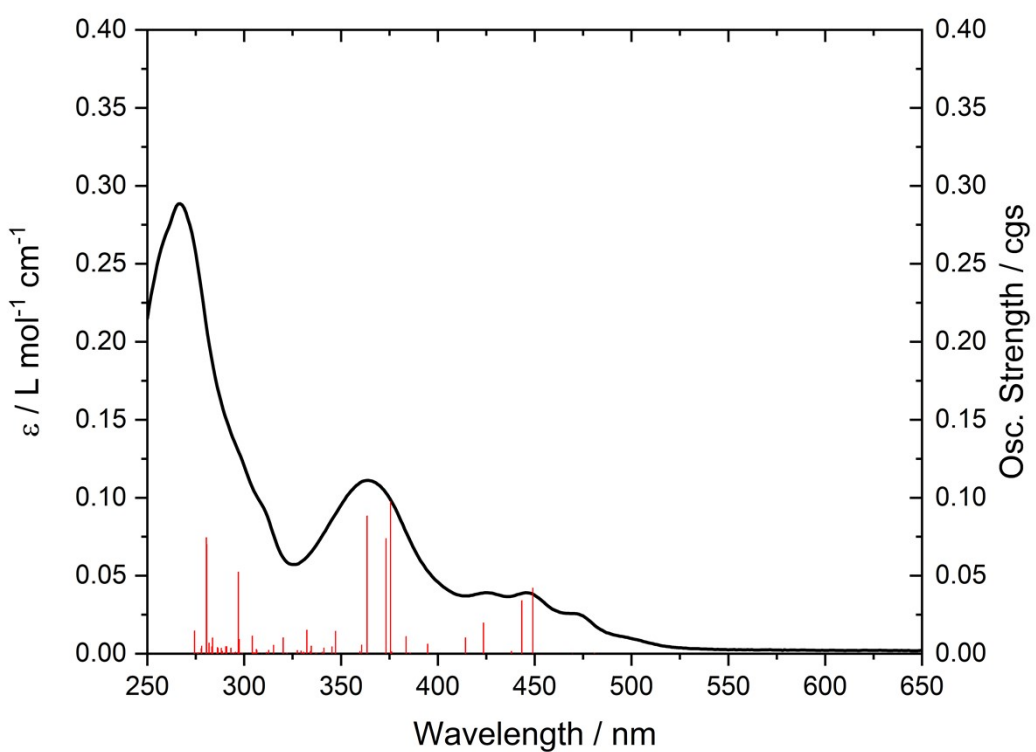


Figure S32. Experimental UV-Vis spectrum of compound **3** in acetonitrile and calculated oscillatory strength of the calculated electronic transitions. a) Full view; b) Zoom view.

Geometries

1

Cr	0.00030435029453	-0.00017921823173	-0.00049039987500
N	-2.33690501176889	1.07453338641386	1.54343861201445
N	1.42021167754291	0.06641599046485	-1.51406696974597
N	1.42009516649813	-0.05722678341546	1.51370684643270
N	2.33652506414530	-1.07103247340930	1.54761055108532
N	-1.41905175054907	-0.07040328779766	-1.51430386441064
N	2.33061672107800	1.08568819930022	-1.54682149288553
N	-2.32947040999390	-1.08972189779818	-1.54509724965039
N	-0.00647124177198	2.11345029297479	-0.00295235841621
N	0.00761741825178	-2.11383361537157	0.00184572279727
N	-1.42036804250698	0.06072034091955	1.51274332120682
C	-1.60109726134686	-0.64270531968421	2.65426867191383
C	1.59954384398627	0.64853842038052	2.65398965361242
C	2.63618670704127	-0.05499484214087	-3.38803305902396
H	3.01234560254262	-0.38916785164203	-4.33860568049301
C	-1.17284506599860	4.18157141273865	0.26108791883780
H	-2.10188352231432	4.68766473434493	0.47601195629188
C	1.14653909533677	-2.79687123507452	0.25138153063932
C	-2.42757082910356	2.04425946984976	0.47137228721253
H	-3.20353732131943	2.74859879817172	0.74450134500887
H	-2.74683381802563	1.54738902558661	-0.44152987828438
C	-2.63537593970796	-0.06414620564550	3.38707700600673
H	-3.00958258512013	-0.39876062706591	4.33826301050327
C	1.12811020607375	2.80393628545001	-0.25186764848613
C	2.42841050279070	-2.04296016020391	0.47769556764389
H	3.20432323354385	-2.74650573711252	0.75300571907730
H	2.74834719876172	-1.54792093511288	-0.43595884483670
C	-1.60448252879049	0.63245104493416	-2.65542307916467
C	3.08335560452259	-1.02221077250337	2.66870787752026
C	-2.41372481780895	-2.06066483566597	-0.47361040587721
H	-3.18479294777447	-2.77014405618854	-0.74732000990819
H	-2.73659810859847	-1.56657667380639	0.43951704182228
C	1.60483290615673	-0.63783268619559	-2.65447341808929
C	-1.14529147768609	2.79735117639127	0.24462675956393
C	2.41508781490573	2.05842100232835	-0.47700576711007
H	3.18653784044103	2.76707063657466	-0.75177688404985
H	2.73749100429962	1.56577946553665	0.43707522117763
C	-1.12651324294178	-2.80522137800358	-0.24670917483573
C	-3.08466142870465	1.02831940756000	2.66403371607060
C	1.14704169436231	4.18827962576077	-0.27097099963382
H	2.07284330717151	4.69988337379384	-0.48684483230121
C	3.07901592847109	1.04145230787862	-2.66707550235465
C	-2.63539264039187	0.04785043812918	-3.38820359985458
H	-3.01195016547075	0.38059298864902	-4.33912100789813
C	-0.01509668298371	4.89187155024801	-0.00559337657824
H	-0.01844962864345	5.97260050973459	-0.00658961847157

C	-0.84166577166289	1.84806404540798	-3.05193483338164
H	-1.09753546491073	2.70368148526904	-2.42849422984877
H	-1.10013745211576	2.09956828565903	-4.07759567343375
H	0.23234353022277	1.70021304787845	-3.00153810038465
C	0.84071967412469	-1.85301431950943	-3.04978865826255
H	1.09623720950150	-2.70846300007124	-2.42600484237624
H	1.09840853256206	-2.10538391490192	-4.07543884751156
H	-0.23315847115887	-1.70425186635333	-2.99892797746669
C	1.17465998439909	-4.18105705575511	0.27013581616154
H	2.10376392455681	-4.68638733927216	0.48657282259070
C	-3.07779486728827	-1.04762593798348	-2.66548896540726
C	2.63336656369166	0.07183520010900	3.38889797664904
H	3.00654600335131	0.40846329963011	4.33977602594454
C	0.82812466232199	1.85955972838741	3.04793193642062
H	1.07819617953989	2.71573588119078	2.42294794202702
H	1.08443766921371	2.11480084021218	4.07321450813818
H	-0.24481833936402	1.70410974432391	2.99748179265814
C	-0.83047442932573	-1.85326121977666	3.05120271578389
H	-1.07919490427022	-2.71021311758443	2.42675526851216
H	-1.08876680821094	-2.10725336109809	4.07629149351362
H	0.24254985698938	-1.69772082748106	3.00260908087383
C	-4.15867218930084	2.00706719884704	2.97213904174765
H	-3.76866259207043	3.02557964592842	2.99496859781053
H	-4.58482705899344	1.77714883239494	3.94507912657256
H	-4.95392655953992	1.96684366053135	2.22628635747401
C	-1.14482294160243	-4.18959623400191	-0.26361810773028
H	-2.07025438961482	-4.70196811187958	-0.47925272566163
C	4.14726498837911	2.02590912703745	-2.97701487095687
H	3.75153381591643	3.04218814698547	-3.00058703249598
H	4.57398858562554	1.79736847431706	-3.95002900219650
H	4.94331034701031	1.99088842486725	-2.23173832924206
C	4.15703044325350	-2.00027853291341	2.98008786754460
H	3.76708196333500	-3.01878291376500	3.00430733632825
H	4.58183735630819	-1.76846747636099	3.95316959618664
H	4.95331063981987	-1.96138121243364	2.23525806866097
C	0.01743142371726	-4.89227035862705	0.00370314931439
H	0.02124591192511	-5.97299789588840	0.00441042443470
C	-4.14592155500946	-2.03278340108520	-2.97364641042079
H	-3.74987829862428	-3.04896293543716	-2.99625375815370
H	-4.57329168299908	-1.80554861102460	-3.94668229586976
H	-4.94152290859922	-1.99713971781796	-2.22792849875097

2

I	12.58196104507405	3.36399154591363	7.24531204989903
I	2.93564970014811	10.68078108987436	4.38389425417440
I	3.61493688681225	7.97824043210413	10.49047994459432
Cr	8.02182188157902	7.47593898995100	6.09193121485771
I	12.94404849298149	7.83352871509917	2.26333023871842
N	9.94533602215487	6.51007087022082	8.18730404998615

N	8.94095206370001	9.08857279591054	7.10952853981209
N	9.31647655366074	7.65025115138610	4.47313576461390
N	7.05476962896736	10.12524643833410	5.06476056543558
N	7.10189862346266	5.86433551651497	5.07335624031893
N	6.21587521580638	5.91199473189722	7.90406008048007
C	4.44534725552077	7.62460512221280	5.29728434641027
H	4.21969337614454	7.20464615496032	4.31476235420954
H	3.50099419255058	7.91746940924100	5.75221556149175
H	4.88857699104917	6.84899850716512	5.90411483049405
N	6.65322096717798	8.84337160088387	5.31824460789714
C	9.87516533212734	7.34335290963595	2.31936820541392
C	5.21555068431614	5.91700350497640	8.80562219840633
C	6.34191168722467	4.85992045038460	3.04394711677289
H	6.25375216633306	4.92068262162624	1.96954262250616
C	10.64941798013025	7.84314761560207	4.37290031862355
N	8.87007709240280	7.35082309140077	3.21631534233234
N	9.45724141764440	6.23013820382499	6.94164685080349
N	6.65844785475090	7.17613280866549	7.63225925949446
C	10.20216312706305	5.21410791249468	6.45495189114045
C	5.01114214238180	7.25258046537372	9.13483872359686
C	9.68185584681035	7.03924229470164	0.88117608947241
H	9.23921270758933	6.05133788832519	0.74734769610594
H	10.64252560101413	7.05922956200468	0.37410906911537
H	9.02693337371465	7.77412597358355	0.41095513227034
C	9.46507298979904	8.91585535347590	8.34316662727295
C	4.53590595219356	4.68513911467928	9.27392889799914
H	4.11976684490378	4.12719070432026	8.43440916192325
H	3.72691523971464	4.95008994923821	9.94888553033116
H	5.23047172544621	4.03366375091364	9.80633605773202
C	10.97996525644223	5.70906090443661	8.50865826770237
C	8.45105002305096	10.50771675840512	5.15562387860297
H	8.51420614546204	11.55763902935537	4.89868815552463
H	9.02396555783257	9.95645942748089	4.41502459403842
C	6.79770864131865	4.75413249706186	7.25135108714305
H	6.28998669224201	3.87918356842178	7.63733792391976
H	7.84449831569383	4.67394258825167	7.53136983876980
C	9.99730893744442	4.55032468483826	5.14223286441087
H	9.35382739284015	3.67589933667215	5.26071991467420
H	10.95484493380368	4.20420931849736	4.75966850688654
H	9.55148168724718	5.20155485843627	4.40438352717117
C	6.95805830164486	5.89231796838930	3.73044151277797
C	5.91739785505056	8.01489800818816	8.38815493320278
C	4.89005033371322	10.10392444187698	4.78606258003176
C	6.15716920228618	12.36331576136475	4.43504978429392
H	6.60848815731869	12.89704576711583	5.27245199916544
H	5.17820967029194	12.79128213839050	4.23867848504755
H	6.78552018568698	12.51385924971874	3.55602630338375
C	6.08539542943108	9.48947992403850	8.44489221412270
H	6.77844171102152	9.75864340112222	9.24483319059825
H	5.12807399182107	9.95394122272737	8.66981839681236

H	6.45735931319946	9.90705382759595	7.52003596306636
C	9.01621603315273	10.30880477306425	6.53433793141457
C	11.02353802204981	7.66116245021536	3.03619438814457
C	6.01488529556397	10.91985160883420	4.74421258472297
C	10.08000180270229	9.95318769912570	9.02304869986714
H	10.49380624616956	9.76944660167391	10.00333818108918
C	9.37286469690811	7.56651530796069	9.00078729042440
H	9.92600938398527	7.58989492865090	9.93162886078772
H	8.34372317140116	7.31438825596206	9.24149260733277
C	11.15807524646858	4.86658853273109	7.41680509866374
C	6.00557181607279	3.74169026045904	5.11914095588894
H	5.63784774972891	2.91304349296463	5.70575546601275
C	9.61168228200240	11.38091347718517	7.17633880580360
H	9.64118866090137	12.34026057302829	6.68172762773626
C	5.31342171496838	8.82057805330975	5.15189420707721
C	11.54858628413020	8.22835346924635	5.49005935937512
H	11.68032866073160	9.31226165151835	5.51018848182966
H	12.52870007896075	7.78293078443743	5.33401562384492
H	11.18116016157702	7.91383739468835	6.45594645110286
C	7.46975765927534	7.07549176411292	2.95654135188395
H	7.37648898856367	6.86653246383157	1.89804262314092
H	6.88112682297731	7.96544157514381	3.16370607378530
C	6.63353948285080	4.79705321103737	5.75757276528342
C	5.85492075232950	3.76869993066853	3.74296060685673
H	5.36823685464425	2.95431669388835	3.22524265897053
C	11.71067000261155	5.79780913055607	9.79621179536969
H	12.14627776859056	6.78902188277993	9.92826077084247
H	12.51058533171009	5.06291261879282	9.81317227367821
H	11.04347408352904	5.60429568959990	10.63732369079390
C	10.15520843128528	11.20549424798321	8.43736547015644
H	10.62811011696325	12.02872954726698	8.95386194206626

3

Cr	8.63122906146343	5.28589767904733	7.73899443009920
N	7.05006305530688	3.85668474538851	7.74187209266907
N	9.49230896166365	4.17736657732771	6.23506212914896
N	9.34637488484008	2.82308412769657	6.17962988037558
N	6.25773966649277	6.26160863590054	9.29323387038391
C	6.88887476692799	7.17868525875560	11.18899273706037
C	10.30242205452704	3.35878561226875	4.27383279036495
C	8.02918441542741	6.82157953229869	10.41612519763091
C	9.32369272274260	7.06580543162964	10.90333157180470
C	5.47578026099228	5.70273954319085	8.20235368726938
C	5.77545600191132	4.24448554106621	7.97266719114121
C	10.08257578590318	4.52774310916458	5.05492046103113
C	5.78616869789423	6.79029264418270	10.41941559889277
C	7.30509419589251	2.54730639045495	7.52386210924605
C	8.72152151883543	2.09920667683458	7.27435401514192
C	9.80665724913695	2.30189981678461	5.04540635148908

C	4.99105579653416	1.99325948653590	7.77354656233221
C	6.29615118351196	1.59921971382408	7.53339695973660
C	10.45921240670138	5.78995720725041	4.56699643625341
C	7.03046801083146	7.77924816680081	12.45452355796449
C	11.24769686440375	4.68121417522624	2.53397835151857
C	9.43376921811870	7.65021127826817	12.14341884323295
C	10.89322952703853	3.43956762755278	2.99841045754174
C	11.03031068509021	5.84120861304907	3.31682869001010
C	4.73208681269290	3.33497550591293	7.99561599487764
C	8.30230583131139	8.00605602598639	12.91747478163429
N	7.61959064473692	6.25905381494771	9.24167364083810
N	10.21239702882981	6.71510784295577	7.74186434958652
N	7.77014297327612	6.39443313070449	6.23507052256407
N	7.91607483010165	7.74871606106592	6.17964206940732
N	11.00472578641651	4.31017661018791	9.29321237096293
C	10.37360195600734	3.39310738404801	11.18897825674618
C	6.96001342294959	7.21302006650573	4.27385051035955
C	9.23328745003159	3.75021828540064	10.41612091810168
C	7.93878227952965	3.50600542934092	10.90334339847574
C	11.78667851861506	4.86904747170333	8.20232816416132
C	11.48700466069420	6.32730310265764	7.97264861875384
C	7.17986974335655	6.04405983327517	5.05493137126382
C	11.47630358259816	3.78149294945956	10.41939125182024
C	9.95736737881597	8.02448687689277	7.52385605197469
C	8.54093798769839	8.47258905454661	7.27436365393303
C	7.45578185727175	8.26990408945739	5.04542447372407
C	12.27140956463427	8.57852696762537	7.77352091667434
C	10.96631346420586	8.97257022347210	7.53338028586936
C	6.80324030427117	4.78184509447863	4.56700247135110
C	10.23201773834021	2.79255958006547	12.45451753553722
C	6.01473109741570	5.89059438819535	2.53399766707855
C	7.82871454776662	2.92161487927051	12.14343824077726
C	6.36919542294160	7.13224076807104	2.99843273517144
C	6.23213109045065	4.73059699226072	3.31684007751694
C	12.53037649200475	7.23681040760935	7.99558980299871
C	8.96018327397609	2.56576643322640	12.91748450119645
N	9.64287416940692	4.31273579466455	9.24166241673980
H	6.95034079700195	3.87898266968984	5.13392381622559
H	5.93831412389459	3.76964483162571	2.91715190320613
H	5.56156075303276	5.78721129605851	1.55816916332791
H	6.20633764059058	8.02478660519352	2.41098310290381
H	7.50977789281877	9.32858001584597	4.85875161149736
H	8.53734372776673	9.52174608669270	7.00023237063630
H	7.93192112369872	8.35319719040690	8.16672633075063
H	10.72114675378599	10.00768157126251	7.34953852430027
H	13.07255568894389	9.30357498992893	7.78687783343302
H	13.53343827697071	6.88741338271900	8.18992793187190
H	12.83009943151398	4.75114056305514	8.47214580282392
H	11.60192329345140	4.28608355372136	7.30342445221762
H	12.53522225752243	3.71794486240812	10.60198554167298

H	11.10307947420829	2.52428527995297	13.03542929570343
H	8.81058388942998	2.10869568169407	13.88547335920391
H	6.84246233935104	2.72712565390195	12.54217622291377
H	7.05637703953781	3.76218899853444	10.34317489797837
H	10.31211984894274	6.69281794882537	5.13392296146038
H	11.32412968342111	6.80216120978481	2.91714307247587
H	11.70085852723393	4.78459969395731	1.55814606835558
H	11.05607813935613	2.54702379773056	2.41095533600428
H	9.75265644731196	1.24322502494919	4.85872888317198
H	9.33054771765129	2.21859284141043	8.16671134123498
H	8.72511249954724	1.05005104526562	7.00021726933640
H	6.54131926900583	0.56410879181442	7.34955473065333
H	4.18991184514723	1.26820913615207	7.78691090040231
H	3.72902554319712	3.68436999285848	8.18996123875458
H	5.66052661229418	6.28570687981122	7.30345045111645
H	4.43236096753896	5.82064264388616	8.47217925427533
H	4.72725120573346	6.85383862181678	10.60201688248955
H	6.15940996783613	8.04752179113231	13.03544115235951
H	8.45191181895173	8.46313922610403	13.88545676095788
H	10.42002429522019	7.84471185845404	12.54214393900975
H	10.20609420555513	6.80962360886747	10.34315657483897

References

- [S1] G. M. Sheldrick, *Acta Crystallogr., Sect. A: Found. Crystallogr.*, 2008, **64**, 112–122.
- [S2] O. V. Dolomanov, L. J. Bourhis, R. J. Gildea, J. A. K. Howard and H. Puschmann, *J. Appl. Crystallogr.*, **2009**, *42*, 339–341.
- [S3] a) F. Neese, *WIREs Comput. Mol. Sci.* **2012**, *2*, 73-78; b) F. Neese, *WIREs Comput. Mol. Sci.* **2022**, e1606.
- [S4] Gaussian 16, Revision A.03, M. J. Frisch, G. W. Trucks, H. B. Schlegel, G. E. Scuseria, M. A. Robb, J. R. Cheeseman, G. Scalmani, V. Barone, G. A. Petersson, H. Nakatsuji, X. Li, M. Caricato, A. V. Marenich, J. Bloino, B. G. Janesko, R. Gomperts, B. Mennucci, H. P. Hratchian, J. V. Ortiz, A. F. Izmaylov, J. L. Sonnenberg, D. Williams-Young, F. Ding, F. Lipparini, F. Egidi, J. Goings, B. Peng, A. Petrone, T. Henderson, D. Ranasinghe, V. G. Zakrzewski, J. Gao, N. Rega, G. Zheng, W. Liang, M. Hada, M. Ehara, K. Toyota, R. Fukuda, J. Hasegawa, M. Ishida, T. Nakajima, Y. Honda, O. Kitao, H. Nakai, T. Vreven, K. Throssell, J. A. Montgomery, Jr., J. E. Peralta, F. Ogliaro, M. J. Bearpark, J. J. Heyd, E. N. Brothers, K. N. Kudin, V. N. Staroverov, T. A. Keith, R. Kobayashi, J. Normand, K. Raghavachari, A. P. Rendell, J. C. Burant, S. S. Iyengar, J. Tomasi, M. Cossi, J. M. Millam, M. Klene, C. Adamo, R. Cammi, J. W. Ochterski, R. L. Martin, K. Morokuma, O. Farkas, J. B. Foresman, and D. J. Fox, Gaussian, Inc., Wallingford CT, **2016**.
- [S5] J. Plasser, *J. Chem. Phys.* **2020**, 084108.
- [S6] N. M. O'Boyle, A. L. Tenderholt and K. M. Langner, *J. Comput. Chem.*, **2008**, *29*, 839-845.
- [S7] E. F. Pettersen, T. D. Goddard, C. C. Huang, G. S. Couch, D. M. Greenblatt, E. C. Meng, T. E. Ferrin, *J. Comput. Chem.*, **2004**, *13*, 1605-1612.
-